Journal of Asian Earth Sciences 277 (2025) 106373

Contents lists available at ScienceDirect

Journal of Asian Earth Sciences

journal homepage: www.elsevier.com/locate/jseaes

Sedimentary records of liquefaction from central Kerala (southwestern India), as earthquake indicators in a cratonic area

Biju John [a,*], Yogendra Singh [a], C.P Rajendran [b]

[a] National Institute of Rock Mechanics, Bengaluru 560 070, India
[b] National Institute of Advanced Studies, Indian Institute of Science Campus, Bengaluru 560 012, India

ARTICLE INFO

Keywords:
Paleo-liquefaction
Sand dikes
India
Craton
Peninsular shield
Earthquake hazard

ABSTRACT

Far from the plate boundaries, the seismogenic zones within the cratonic areas of Indian land mass had remained largely undetected. The moderate earthquakes in such areas have proved to be hugely damaging because of their infrequency and consequent lack of societal preparedness. As the subtle geological expressions of tectonism make identifying hazardous zones in cratonic areas difficult, it is important to develop locally appropriate geological criteria to isolate potential seismic source zones. Although seismically induced liquefaction preserved in the sedimentary sections is useful as an earthquake proxy, its scope remains underestimated in cratonic regions. Here we offer a field-based methodological approach to mapping liquefaction features from such an area, located south of the Bharathapuzha River in the southwestern part of the Indian craton. We used the field data to constrain the near-field earthquake potential. The earthquake-induced soil liquefaction, in the form of sand dikes and sills, was identified within an area of roughly 100 km^2, and the available data suggest two episodes of liquefaction – the one between 2.0 ka and 2.5 ka, and a later event around 0.78 ka BP. The spatial distribution and the dimension of the soil liquefaction features, in an area known for the occasional spurt in minor earthquakes in recent times, are suggestive of a potential seismic source in the region that can generate earthquakes of moment magnitudes (M_w) ranging from 5.5 to 6.5. Thus the present observation is a vital input for constraining the region's seismic hazard and the methodology developed here can be used in other areas of unknown potential.

1. Introduction

The cratonic region of the Indian landmass was long held to be seismically stable (Johnston, 1989). Some damaging earthquakes in peninsular India in the last few decades (e.g., the 1993 Killari, M_w 6.3; 1997 Jabalpur, M_w 5.7; and 2001 Bhuj, M_w 7.7) have partly transformed this widely held view. Earthquakes reported from other cratonic parts of the world (eastern and central North America, Africa, Australia, Brazil, Greenland, and Antarctica) indicate reactivation of the associated older fault systems at varying periods (e.g., Sykes, 1978). Since many of the faults in these regions have never been reactivated during recorded history, earthquakes may recur as a total surprise. In those regions, the historical information on earthquakes is either sparse or non-existent to determine the magnitude-recurrence relationship for damaging earthquakes, and therefore inherit a huge risk from out-of-the-blue event/s. For example, the devastating Killari (M_w 6.3) earthquake was considered as an 'out-of-blue' event although it was later discovered that it occurred on a fault that shows geological evidence of faulting (Rajendran et al., 1996). Likewise, although the rift zones of Narmada and Godavari are prominent tectonic structures in the Indian craton, and known to be seismically active, the lack of geological information on previous damaging earthquakes precludes realistic understanding of the maximum magnitude earthquakes possible for those regions (Khan et al., 2013; Rajendran and Rajendran, 2022).

Paleoseismology, or the study of fault rupture, ground shaking and other earthquake effects as preserved in the geologic record, extends our knowledge of seismic activity into the prehistoric period and thereby improves our understanding of the long-term behaviour of fault zones or earthquake sources (Tuttle, 2001). The key element of seismic hazard assessment is source characterization, that is, the assignment of magnitudes and recurrence rates for large, potentially damaging earthquakes. Thus, at many global localities (from tectonically active plate margins to cratonic areas and mountain belts), such studies for identifying prehistoric earthquakes in region-specific seismic hazard

* Corresponding author.
E-mail address: b_johnp@yahoo.co.in (B. John).

https://doi.org/10.1016/j.jseaes.2024.106373
Received 15 May 2024; Received in revised form 29 September 2024; Accepted 18 October 2024
Available online 31 October 2024

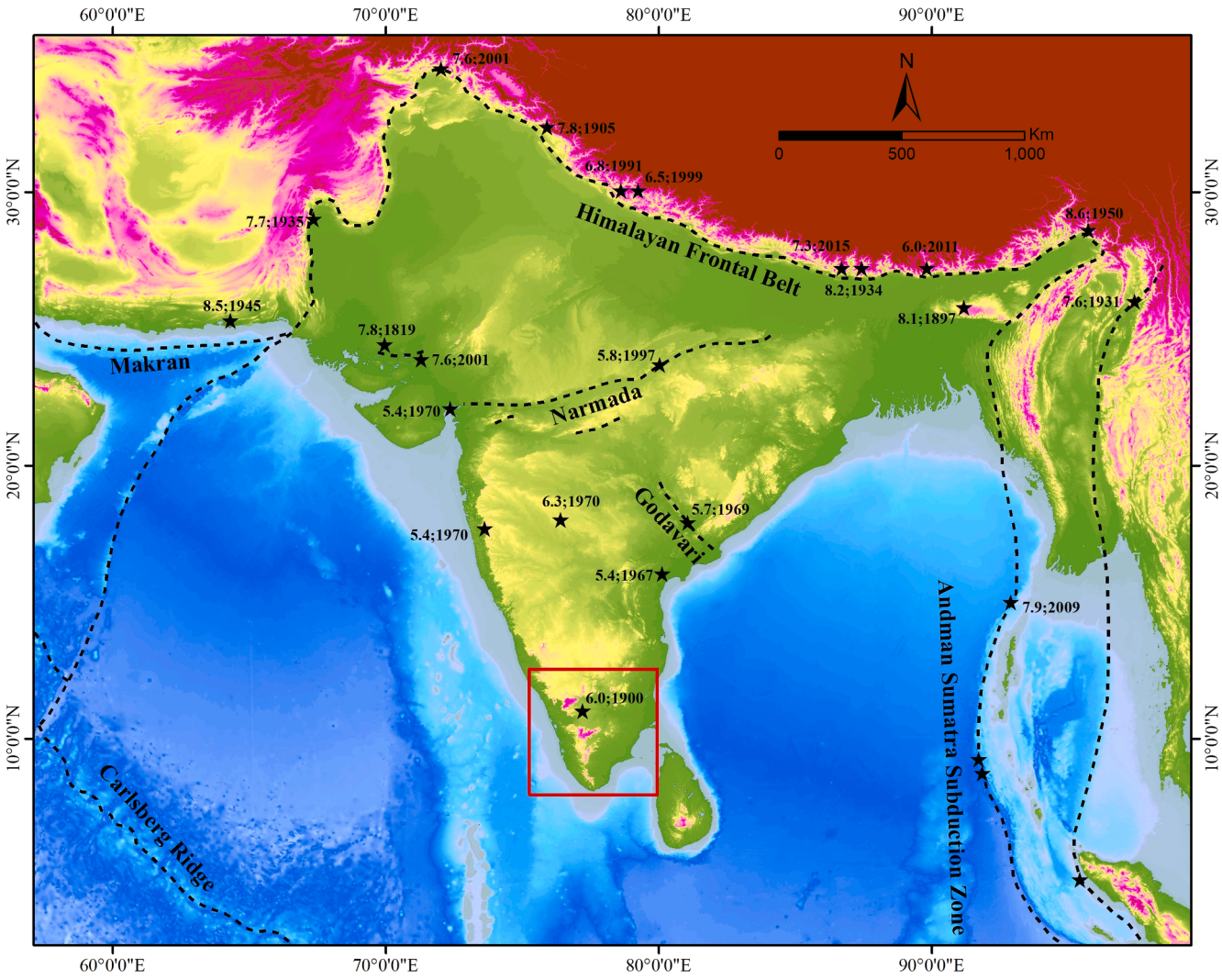

Fig. 1. Map showing significant structural features surrounding Indian land mass. Locations of major faults, namely, Narmada and Godavari and earthquakes of the continental shield are marked. The study area is located within the square shown at the southern part of Indian peninsula.

evaluation have gained prime importance (e.g., McCalpin, 2009). Occurring as both on-fault and off-fault features, liquefaction evidence is considered a potential tool for magnitude estimation of pre-instrumental and prehistoric earthquakes (Galli, 2000; Tuttle, 2001; Castilla and Audemard, 2007; Świątek et al., 2023).

Earthquake-induced soil liquefaction is triggered when saturated, granular sediment temporarily loses its strength due to earthquake ground shaking (Seed and Idriss, 1982). Besides the usefulness of liquefaction phenomena for soil engineering, over the last 30 years, paleoseismic studies have also focused on the preserved liquefaction features in sedimentary sections as earthquake proxies for constraining the frequency and magnitude of earlier earthquakes, as they provide valuable clues on the strength of shaking or spatial extent of ground failure of the causative earthquakes (McCalpin, 2009). The study of the liquefaction potential of moderate earthquakes gained importance after Holzer et al. (2010) published the results of the 2009 California with a magnitude of M = 5.2 earthquake, which generated extensive liquefaction within 1.2 sq. km, where the source bed for liquefaction was located at a shallower depth (<2m). In a review of historical observations of earthquake-triggered liquefaction, Green et al. (2019) found that earthquakes of moment magnitude 4.5 could trigger liquefaction in extremely susceptible soil conditions. The host of studies conducted since then have enabled the researchers to develop various empirical relations between observed liquefaction with the causative intensity and/or magnitude.

There has been steady progress in paleoseismological research in India over the last few decades (Rajendran et al., 2020) – mostly focused on the western and eastern Himalayas – one of the youngest and most active plate boundaries. These studies are targeted at the primary fault ruptures (e.g., Kumar et al., 2006) as well as the earthquake proxies such as liquefaction features of past earthquakes (Rajendran et al., 2016; Fig. 1). Extensive studies carried out along the Himalayan Frontal Thrust (HFT) have provided significant insights into rupture patterns and spatiotemporal distribution of major earthquakes. Much work has also been conducted in the intraplate region of Gujarat, NW India where major earthquakes have occurred by reactivation of intra-basinal faults linked to an older rift (e.g., Rajendran and Rajendran, 2001). Significantly, a study conducted in western India, on the Tapti fault, adjacent to the western part of the Narmada rift reported an offset alluvial fan surface that resulted from one or more magnitude 7.6–8.4 thrust-faulting earthquakes, in the Holocene, and hence holds potential to produce damaging earthquakes in the future (Copley et al., 2014). Though much of the paleoseismic research in India has been focused on identifying active zones within the inter-plate and passive rift settings, some studies have also focused on the southern part of Indian craton (e.g., John and Rajendran, 2009; Praseeda et al., 2015; Singh et al., 2016a; Singh et al., 2016b; Fig. 2).

Of relevance to the present discussion, a few studies were conducted

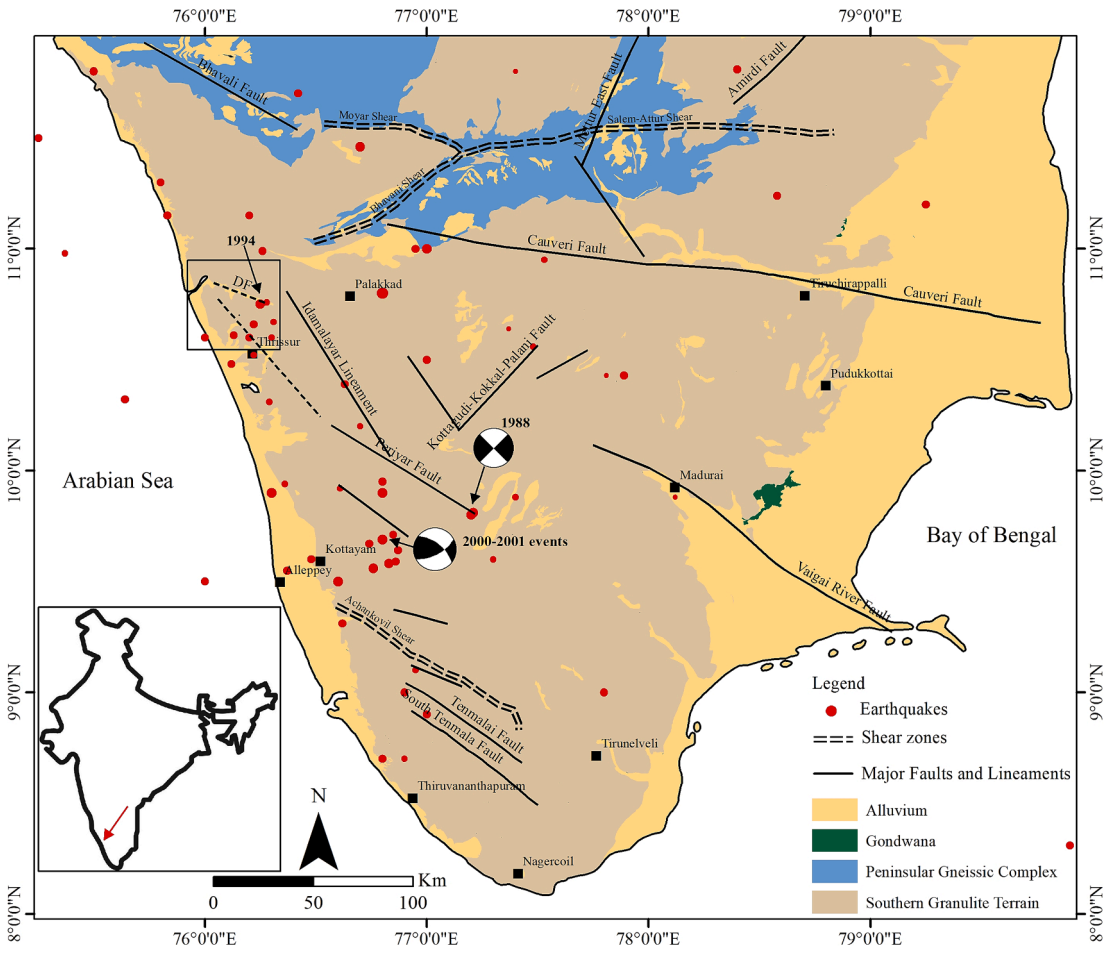

Fig. 2. Seismotectonic map of peninsular India showing the major shear zones, namely, Achankovil, Moyar and Salem-Attur and associated structural features (GSI, 2000); Geology is adapted from the (Bhukosh portal of GSI 2019). Earthquake and some of the fault locations are sourced from Rajendran et al. (2009); John and Rajendran (2009); Rajendran et al. (2009); Praseeda et al. (2015); Singh et al. (2016b). Fault plane solutions for the 1988 Idukki and 2000–2001 earthquakes are adapted from Rastogi et al., (1988) and Bhattacharya and Dattatrayam (2002), respectively. The study area marked a rectangle includes trends of the Desamangalam fault (DF) and the Periyar fault. Inset: Outline map of India the red arrow points to the study area.

in the vicinity of Palghat–Cauvery shear zone within the Precambrian crystalline terrain of southern India, where low-level seismicity has been reported, since 1989 (Fig. 2). Initially John and Rajendran (2008) identified anomalies in drainage network of the area attributed to a neotectonically active fault (Rao et al., 2002), which resulted in a sharp turn at Desamangalam to the east to west flowing major river (the Bharathapuzha River; see Fig. 3). The studies by John and Rajendran (2009) on a fault exposure (named as the 'Desamangalam' fault) identified four episodes of movement with an accumulated dip/oblique slip of > 2.1 m in the reverse direction, indicating a possible characteristic slip of ~ 52 cm (for each event; see supplementary material for details). Based on the empirical relationships derived by Wells and Coppersmith (1994), using average displacement and fault length, this fault is considered capable of generating $M > 6$ earthquakes (see supplementary material).

A later study identified signatures of another fault zone located south of the Desmangalam fault, which has influenced/controlled the river courses (reflected as sharp turns and meanderings) of smaller drainages in the area (Singh et al., 2016a; Singh et al., 2016b). This fault is considered as an offshoot of the regional structure called the Periyar fault and its southern zone is marked by low-level seismicity (Fig. 2; John et al., 2016). The low-level seismicity and the structurally controlled drainage network in the area prompted us to investigate the local sedimentary sections within alluvial plains between Bharathapuzha and Wadakkanchery Rivers (see Fig. 3 for location) for liquefaction features induced by the possible previous earthquakes. This article presents an inventory of such sedimentary features in the region and their chronology. These findings have implications for the seismic hazard potential for the region.

2. Regional Setting

The southern peninsular India is part of a complex polyphase deformed segment of the Precambrian crust, known as the Southern Indian Shield (Ghosh et al., 2004). The most important Precambrian deformation belts of the region are known in the geological literature as the Moyar–Bhavani (MBSZ), the Palghat–Cauvery (PCSZ) and the Achankovil (AKSZ) shear zones (Fig. 2). The studies identified the PCSZ as an E–W trending shear zone running from east to west in the southern part of peninsular shield, forming an ~ 40 km-wide mountain pass in the Western Ghats. The Gap also hosts the Cauvery and Bharatapuzha Rivers in the eastern and western parts, respectively (Drury et al., 1984; Ramakrishnan, 1993). Identified as a shear zone (Arogyaswami, 1962; Drury et al., 1984; Subramaniam and Muraleedharan, 1985; D'Cruz et al., 2000), the 'Palghat Gap' provides evidence of the youngest phase of Precambrian deformation in the form of pseudotachylite that was dated at 895 ± 17 Ma (Bhaskar Rao et al., 2006).

The E–W lineaments are the most pervasive regional structural trends within the Palghat Gap and the E–W flowing segment of the Bharathapuzha River follows one such lineament (John and Rajendran, 2009). Occasional low-level seismic events have been reported in this

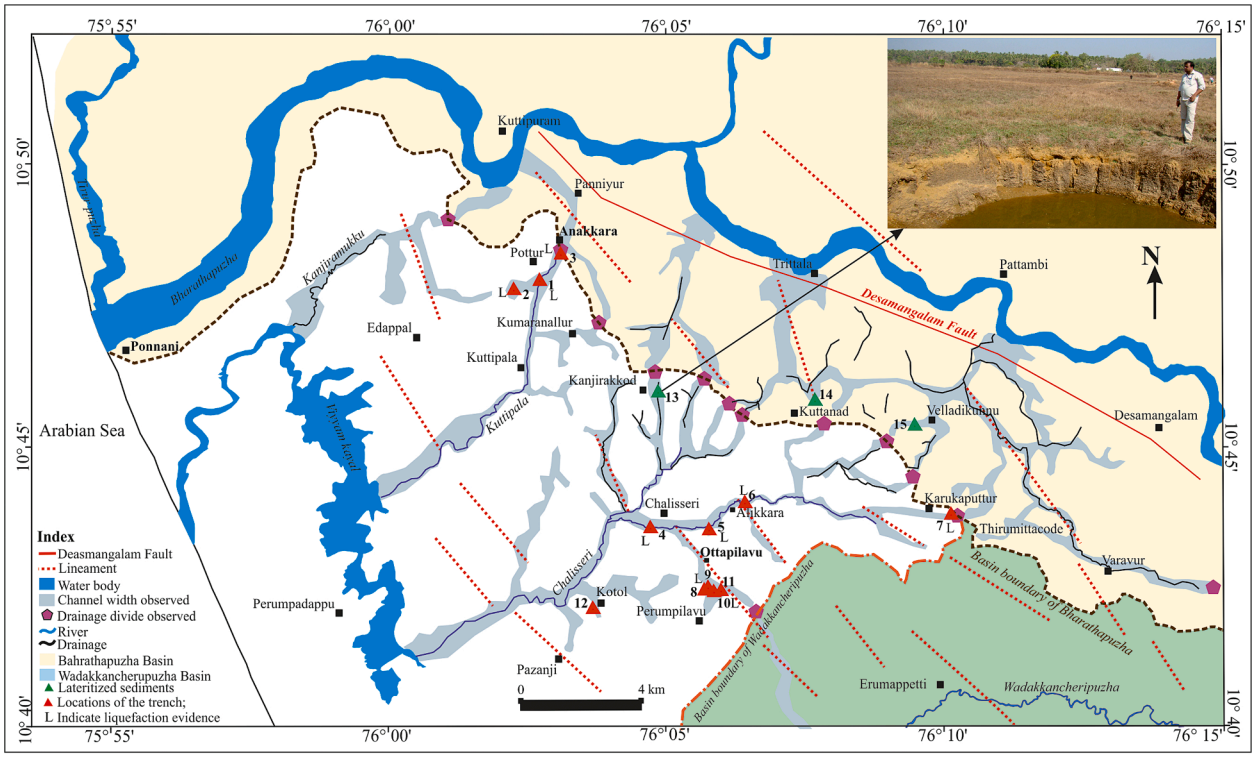

Fig. 3. Study area showing lineaments, and the channels observed between the Bharathapuzha and Wadakkancheripuzha Rivers. The southern basin boundary of the Bharathapuzha River is marked in dashed lines. The triangles represent the locations of the trenches described in the text; 'L' indicates the location of paleo-liquefaction features. Inset: Exposure at Kanjirakkod (Site13), showing indurated lateritised sediments with thin soil cap located close to the basin boundary of the Bharathapuzha River. Note the vertical fractures within the indurated part of lateritised sediments.

Table 1
Trench locations of the present study. The dimensions of the excavations are indicated as length (L), width (W) and depth (D) in meters. Serial No 1–12 are excavated during the studies and the rest are the studied excavations observed/available during the field work. Observation of paleoliquefaction features is mentioned in the last column.

S. No	Location	Lat/ Long	Excavation LxWxD (m)	Observation on liquefaction
1	Site 1-Pottur Temple	10°48′0.01″N 76° 2′34.85″E	2.0 × 0.92 × 3.3	Yes
2	Site 2-Pottur West	10°47′50.23″N 76° 2′8.01″E	2.95 × 0.92 × 2.3	Yes
3	Site 3-Anakkara	10°48′36.27″N 76° 3′1.38″E	2.58 × 1 × 1	Yes
4	Site 4-Chalissery – West	10°43′42.53″N 76° 4′36.94″E	2.5 × 0.92 × 2.1	No
5	Site 5-Chalissery – East	10°43′39.51″N 76° 5′31.48″E	2.9 × 0.92 × 2.25	No
6	Site 6-Alikkara	10°44′5.86″N 76° 6′29.94″E	3.9 × 2 × 1.2	Yes
7	Site 7-Thirumittacode	10°43′53.41″N 76° 9′55.61″E	2.8 × 1 × 2.7	Yes
8	Site 8-Perumpilavu	10°42′38.33″N 76° 5′39.24″E	4 × 3 × ~ 3.5	Yes
9	Site 9-Perumpilavu	10°42′38.33″N 76° 5′40.06″E	2 × 2 × 1	Yes
10	Site 10-Perumpilavu	10°42′27.18″N 76° 5′46.92″E	2.9 × 1.5 × 1.8	Yes
11	Site 11-Perumpilavu	10°42′37.68″N 76° 5′41.24″E	2.9 × 1.5 × 2.3	Yes
12	Site 12-Kotol	10°42′21.50″N 76° 3′36.66″E	2.85 × 1.42 × 2.9	No
13	Site 13-Kanjirakkod	10°45′59.86″N 76° 4′49.72″E	Circular pit of 6 m diameter and 1 m deep.	No
14	Site 14-Kuttanadu	10°46′0.36″N 76° 7′30.06″E	An artificial pond 10x10x5	No
15	Site 15-Velladikunnu	10°45′25.58″N 76° 9′35.04″E	Open well of 4 m diameter and 20 m deep	No

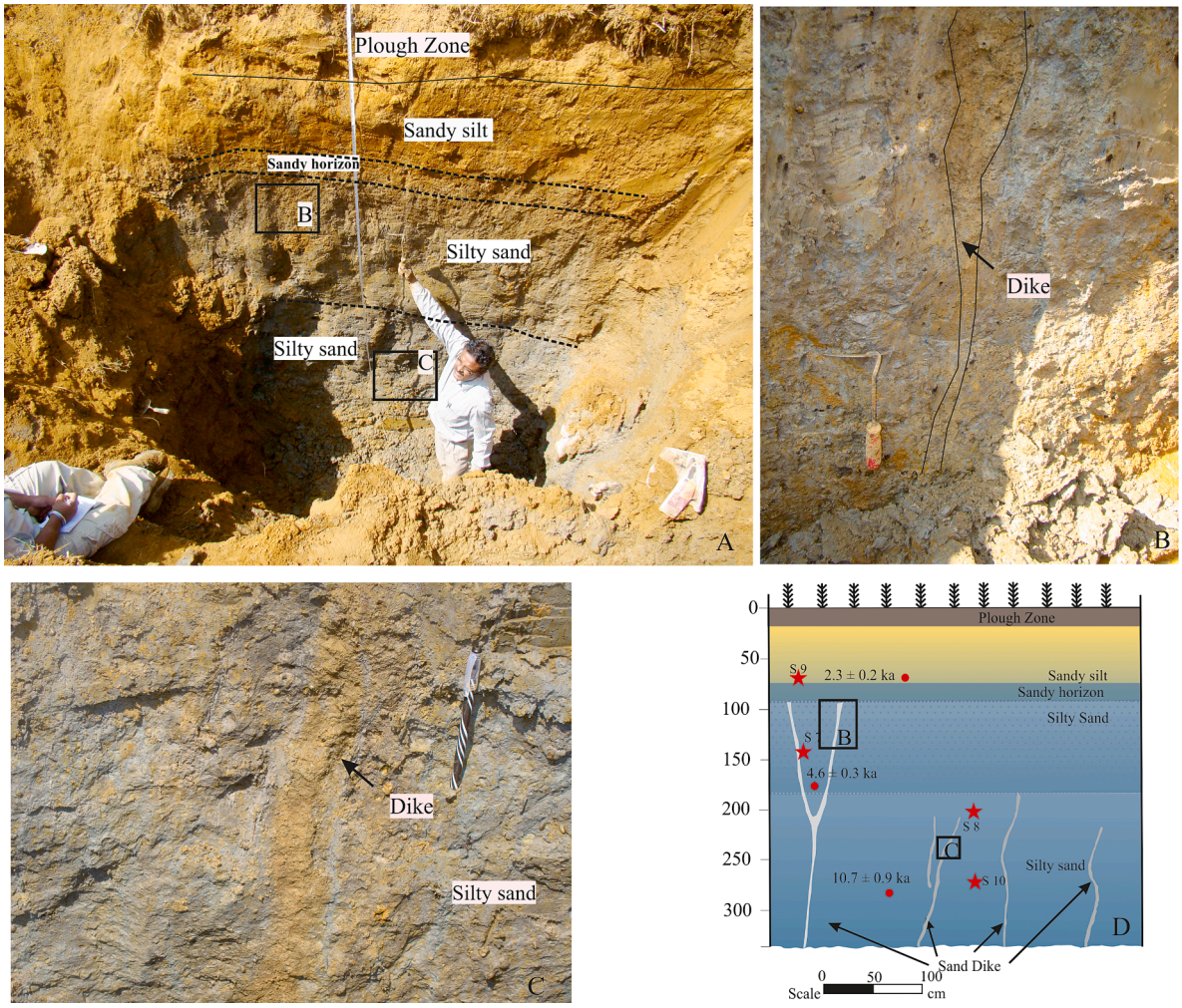

Fig. 4. Observations from the trench from Site 1 (Fig. 3 for location). A. View of the 3,3-m-deep trench showing different litho-units, rectangles showing the location of the figures B & C; B. Irregular dark sand unit observed between sandy silt and silty sand; C. Closeup view of one of the dike observed in the trench, note the dark colour with very feeble contrast with the host (silty sand). D. Sketch representing the trench wall studied, showing closely spaced dikes with some of them branched upward.

Table 2
Details of paleoliquefaction sites. The locations of the trenches as numbered in Table 1. The depth of excavation, the thickness of the sand dikes observed and height of dikes observed in trenches are expressed in centimetre. The number of dikes observed in each excavations is also given.

S. No	Location	Depth of excavation (cm)	Number of dikes observed	Thickness of dike (cm)	Visible height of dike/s (cm)
1	Site 1	330	4	2.5–4	120–240
2	Site 2	230	3	4–5	~64
3	Site 3	100	3	8–12	~72
4	Site 6	120	4	2.3–6	35–41
5	Site 7	270	1	~3.3	226
6	Site 8	350	8	12–25	90–300
7	Site 10	180	2	21.8–23.3	42–48
8	Site 11	230	2	20.1–20.7	94–108

area since 1989. The field studies conducted in the epicentral area of the 2nd December 1994 (M = 4.3) earthquake near the town of Wadakkancheri, identified a > 30 km long NW-SE trending south dipping (45°) structural feature. Named after local village 'Desamangalam' this fault, as surmised by John and Rajendran (2008), may have influenced the drainage pattern of the area. The reverse movements on this fault resulted in forcing the originally E-W flowing Bharathapuzha River to shift its course in a SE- NW direction, as it reached the Desamangalam area.

The present study area is located between the southern side of the main trunk of the Bharathapuzha River and another small river (called Wadakkancheripuzha), located further south within the southwestern terminus of the Palghat-Cauvery shear zone (Fig. 2). Three west-flowing channels, roughly parallel to each other, are identified as misfit drainages (having narrow drainage along a wide valley) between the Bharathapuzha and Wadakkancheripuzha Rivers and abut against the coast parallel estuarine water body (called locally as Viyyam Kayal; Fig. 3). For discussion in this paper, these channels are called Kanjiramukku, Kuttipala and Chalisseri drainages, (Fig. 3).

A part of the coastal wetlands, the Viyyam Kayal (estuary) is separated from the sea by coast parallel sandbars (Fig. 3). The formation of coastal wetlands owed to the land-sea interactions during the mid-Holocene interval (Alappat et al., 2021). It is suggested that the misfit channels that join Viyyam Kayal, as distributaries of the Bharathapuzha River, are deprived of their headwaters due to the movement of the hanging wall block of the Desamangalam fault (John et al., 2013). The morphometric analysis has also identified another segmented fault system (extension of the Periyar fault) on the southern side of the Desamangalam fault (Fig. 2), which induced subtle landform modifications (Singh et al., 2016a; Singh et al., 2016b). The segments of these

Table 3
The details of samples collected for grain size analyses. The location of the trench from the coast and Desamangalam fault is given in kilometer.

Trench location	Distance from the coast	Distance from Desamangalam fault	Sample No	Sample description
Site 1	14 km	4.25 km	7	Dike material at 120 cm depth
			8	Clay sample at 2 m depth
			9	Sand mix soil at depth 70 cm
			10	Clay mix sand at 270 cm depth
Site 2	13 km	4.75 km	3	Trench Material sand mixed soil (more percentage of soil) at depth 70 cm
			4	Trench Material sand mixed soil at depth 90 cm
			5	Spout Material 150 cm depth
Site 3	15 km	2.75 km	6	Dike material Annakare trench
Site 7	23 km	5.5 km	11	Dike material Thirumttacode trench
Site 8	15 km	11 km	2	Fresh grey-white sand from Peumpilavu well
Site 9	15 km	10.75 km	12	Sand Sample collected the open excavation opposite to Perumpilau well
Site 10	15 km	10.5 km	1	Spouted Material from the trench at depth 1.2 m

lineaments/faults influenced smaller drainages on the southern side of the Wadakkancheripuzha River and are also associated with brittle faulting. Thus, the earlier studies suggest neotectonic activities near the present study locations. Here we report the results of our field examination of the Late Holocene sedimentary sections in the area exposed along the channel valleys, identified between the Bharathapuzha and Wadakkancheripuzha Rivers and discuss the tectonic implications of the findings.

3. Methods followed in the present study

We demarcated drainage basins between the Bharathapuzha and Wadakkancheripuzha Rivers using topographic maps of 1: 50,000 scale. Landsat and LISS-IV data were used to mark the channels and their connectivity and to identify suitable sites for detailed investigations. Our investigations were focused on the nature of lithology/sediments observed in these channels through shallow trenches (Fig. 3). These channels, where they debouch into the shore/coast parallel water body (Viyyam Kayal) are in waterlogged condition (wetland) throughout the year. Thus, the study had to be conducted along the channel segments away from the water-logged area (Fig. 3). The study used mechanized trenching using a backhoe as it helps in quick excavation before the pits get flooded since the local water table was very shallow. The trenches made close to Viyyam Kayal, even in the months of winter, could not progress beyond 1 m depth because of the shallow water table. The exposed walls were then cleaned for a detailed mapping of the sedimentary units. The walls of the trenches were mapped, and sediment samples were collected for grain size analysis. The OSL (Optically Stimulated Luminescence) dating of the samples from confining layers helps to minimize the exposure error. Sediment samples from within the sand dikes are useful for determining the age of the deposit liquefied (age of the source sand).

The basin boundary of the Bharathapurza River demarcated in the south is exceptionally straight, extending in an NW-SE direction, parallel to the main trunk of the river, which overlaps with the trend of the Desamangalam fault, as discussed earlier. Drainages directed on either side of this basin boundary are marked by narrow width within a broad valley and many of them have a counterpart on the other side. Close to the basin boundary, we observed thin sedimentary layers sitting over the lateritised formation (Fig. 3).

4. Results

The trenches along the Kuttippala and Chalisseri channels (see Fig. 3) exposed thick clay, whereas the inland (>10 km from the coast) ones revealed coarser sediment. Many of these trenches showed that the overlying young sediments are underlined by partially lateritised sedimentary formation. The overlying younger sediment's thickness is found to be decreasing considerably as we move upstream towards the basin boundary of the Bharathapuzha River. The indurated surface of

Table 4
Data on Quartz Optically Stimulated Luminescence (OSL) dating from the trenches. The sample depth (in centimetre) and location of the trench are also given.

Sr No	Lab No.	Depth (cm)	Palaeodose(Gy)	Dose rate (Gy/ka)	Age(ka)	Location
1	LD1475	90	4.71 ± 0.41	2.1 ± 0.1	2.3 ± 0.2	Site 1
2	LD1474	180	10.04 ± 0.41	2.2 ± 0.1	4.6 ± 0.3	10°48′0.01″N, 76° 2′34.85″E
3	LD1473	300	24.42 ± 1.5	2.3 ± 0.1	10.7 ± 0.9	
4	LD-1831	90	2 ± 0.2	1.06 ± 0.1	2 ± 0.1	Site 2
5	LD-1830	150	3 ± 0.3	1.0 ± 0.1	3 ± 0.3	10°47′50.23″N, 76° 2′8.01″E
6	LD-1875	170	1.6 ± 0.3	0.6 ± 0.02	2.7 ± 0.5	
7	LD3580	260	5 ± 0.1	3.1 ± 0.2	1.5 ± 0.1	Site 410°43′42.53″N76° 4′36.94″E
8	LD3583	100	11 ± 0.3	2.4 ± 0.2	4.5 ± 0.3	Site 510°43′39.51″N76° 5′31.48″E
9	LD3585	110	0.7 ± 0.2	0.83 ± 0.05	0.5 ± 0.05	Site 610°44′5.86″N, 76° 6′29.94″E
10	LD3579	90	4.2 ± 0.1	1.68 ± 0.4	2.5 ± 0.1	
11	LD-1833	42	3.4 ± 0.2	1.8 ± 0.1	2 ± 0.1	Site 710°43′53.41″N, 76° 9′55.61″E
12	LD-1832	60	5 ± 0.4	2.0 ± 0.1	2.5 ± 0.2	
13	LD1472	250	4.89 ± 0.43	0.8 ± 0.1	7.0 ± 1.1	Site 810°42′38.33″N, 76° 5′39.24″E
14	LD-1876	50	1 ± 0.1	1.3 ± 0.06	0.7 ± 0.08	Site 910°42′38.33″N, 76° 5′40.06″E
15	LD3578	120	3.1 ± 0.5	0.7 ± 0.03	4.4 ± 0.8	Site 1010°42′27.18″N76° 5′46.92″E
16	LD3582	150	1.7 ± 0.4	0.55 ± 0.02	3.1 ± 0.7	Site 1110°42′37.68″N76° 5′41.24″E

Note. Optically Stimulated Luminescence (OSL) measurements were carried out Riso TL/DA-20 Reader, Denmark with a blue light emitting diode (LED) source which is located in Wadia Institute of Himalayan Geology, Dehradun, India. About 35–38 aliquot from quartz grains (size fraction 90–125 μm), were prepared per sample and the Single Aliquot Regeneration (SAR) protocol (Murray and Wintle, 2000) was used for equivalent dose (De) determination. The equivalent dose (De) value is calculated for each aliquot by Duller's Analyst software (using initial integral (0.8sec) of the OSL) and weighted mean value of the De is used for age calculation. For the dose rate estimation, concentration of uranium, thorium, and potassium in the sediments were measured by ICP-MS or XRF. The water content was determined for all the samples by heating at 100 °C. The Single Aliquot Regeneration protocol (Murray & Wintle, 2000) was used for equivalent dose (ED) determination. Further details of optical dating techniques can be obtained from Aitken (1998).

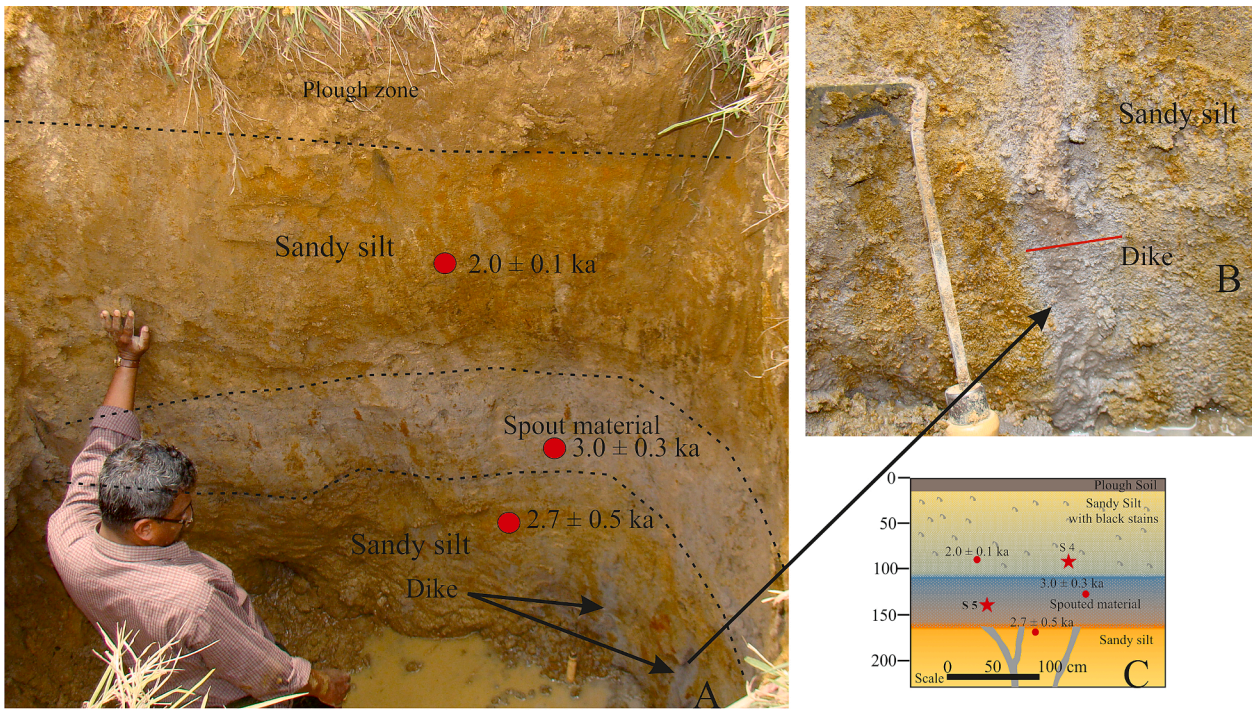

Fig. 5. Observations from Site 2. A 2.4-m-deep trench west of Site 2 showing a liquefaction feature. A. View of the trench showing different litho-units, sand dikes and spouted sand showing variable thickness B. Closeup of sand dike C. Sketch showing lithology and dikes. Red circles are OSL sample locations and red stars are samples taken for grain-size analysis.

lateritised sediments observed close to the basin boundary is also marked by fracturing parallel to the trend of the river (Fig. 3A). The trench stratigraphy of various sites situated along both the Kuttippala and Chalisseri valleys/channels are discussed in the following sections.

4.1. Site 1 (Pottur temple)

A trench was made in the N-S trending Kuttippala valley, which must have hosted a now defunct channel and the area is currently under paddy cultivation (Table1; Fig. 3). The topography suggests that the flow trends southward. The water table was shallow, and the infiltration occurred below 2 m. The 3.4 m deep trench (Fig. 4A) which exposed sand dikes (Table 2; Fig. 4B & 4C) had a 15–20-cm thick plough zone at the top, followed by ~ 80 cm thick reddish sandy silt (Fig. 4D). Irregular patches of sand were seen below this sandy silt (Fig. 4B), are and underlain by ~ 1 m thick dark silty sand (Table 3; Fig. 4A & 4D). Greyish-colored silty sand is the lowermost unit observed in the trench, which provided an OSL date of 10.7 ± 0.9 ka, and the overlying dark silty sand was dated at 4.6 ± 0.3 ka (Table 4; Fig. 4D). The OSL date of reddish sandy silt observed below the plough zone was 2.3 ± 0.2 ka. Thin tubular-shaped dikes, of the order of 2.5–4 cm thick, were observed to be cutting across the silty sand (Table 2; Fig. 4C & 4D). Two sets of sand dikes were observed in the section – one set carrying dark-coloured sediment (Fig. 4 C) with some amount of silt content (Table 3; Fig. 16), and the other set with light-coloured fine to medium sand (Fig. 4B). Some of these dikes appeared as though they were branching upward.

The section stratigraphy suggests that the liquefied sand had been emplaced through relatively impervious thick silty sand units exposed at the bottom of the trench. Although the continuity of the dikes with dark-coloured silty sand was only confined to the lower part of the silty sand unit, the dikes observed with light-coloured sand had been emplaced through the upper part of the silty sand (Fig. 4B). The sandy layer above the silty sand unit could be part of the spouted material during the liquefaction event. Since this layer appeared sandwiched between the sedimentary units dated 2.3 ± 0.2 ka (sandy silt) and 4.6 ± 0.3 ka (silty sand) respectively, the liquefaction event might have occurred before the deposition of sandy silt. The textural difference between the two sets of dikes indicates the possibility that they might have formed during two events or that the emplaced sand belonged to different sediment sources.

4.2. Site 2 (Pottur west)

The trench site is located southwest of Site 1, as described earlier on a NE-trending short valley/channel (Table 1; Fig. 3) and is located ~ 1 km (aerial distance) from the earlier site. The shallow water table hindered the inspection of the deeper part of the section below 2.3 m (Fig. 5A, B & C). The trench exposed a 15–18 cm thick plough zone at the top and is underlain by a mottled layer of fine sandy silt of ~ 1 m thick. A layer of white sand was observed below this layer (Fig. 5A & 5C). The thickness of this unit appeared to be reducing laterally (the maximum thickness observed is 55 cm). The sandy silt (>64 cm thick) observed at the bottom of this unit appeared mixed with coarse sand (Table 3). The lower part of this layer was mostly silty. The mottled fine sandy silt layer observed below the plough zone was dated 2.0 ± 0.1 ka (Table 4; Fig. 5A & C). The sand unit observed below was dated 3.0 ± 0.3 ka and the sandy silt layer at the base was dated at 2.7 ± 0.5 ka. At the bottom level, a couple of 4–5 cm-thick sand dikes (Fig. 5B) could be observed (Table 2). The texture of the sedimentary material within these sand dikes and in the overlying white sandy layer appeared similar. The dikes were slightly thicker than the one observed in Site 1, although one was a branching type.

The liquefaction event identified here had impacted the base sandy silt units at the lower part of the trench (Fig. 5A). Since this layer sandwiched between the sedimentary units provided OSL dates of 2.0 ± 0.1 ka (sandy silt) and 2.7 ± 0.5 ka (silty sand), the liquefaction event is assumed to have been occurred earlier than the formation of units that provided the date 2.0 ± 0.1 ka (Table 4). As the age data suggest, the white sand unit may have formed around 3.0 ± 0.3 ka, and the sand emplaced from below may not have been exposed to sunlight.

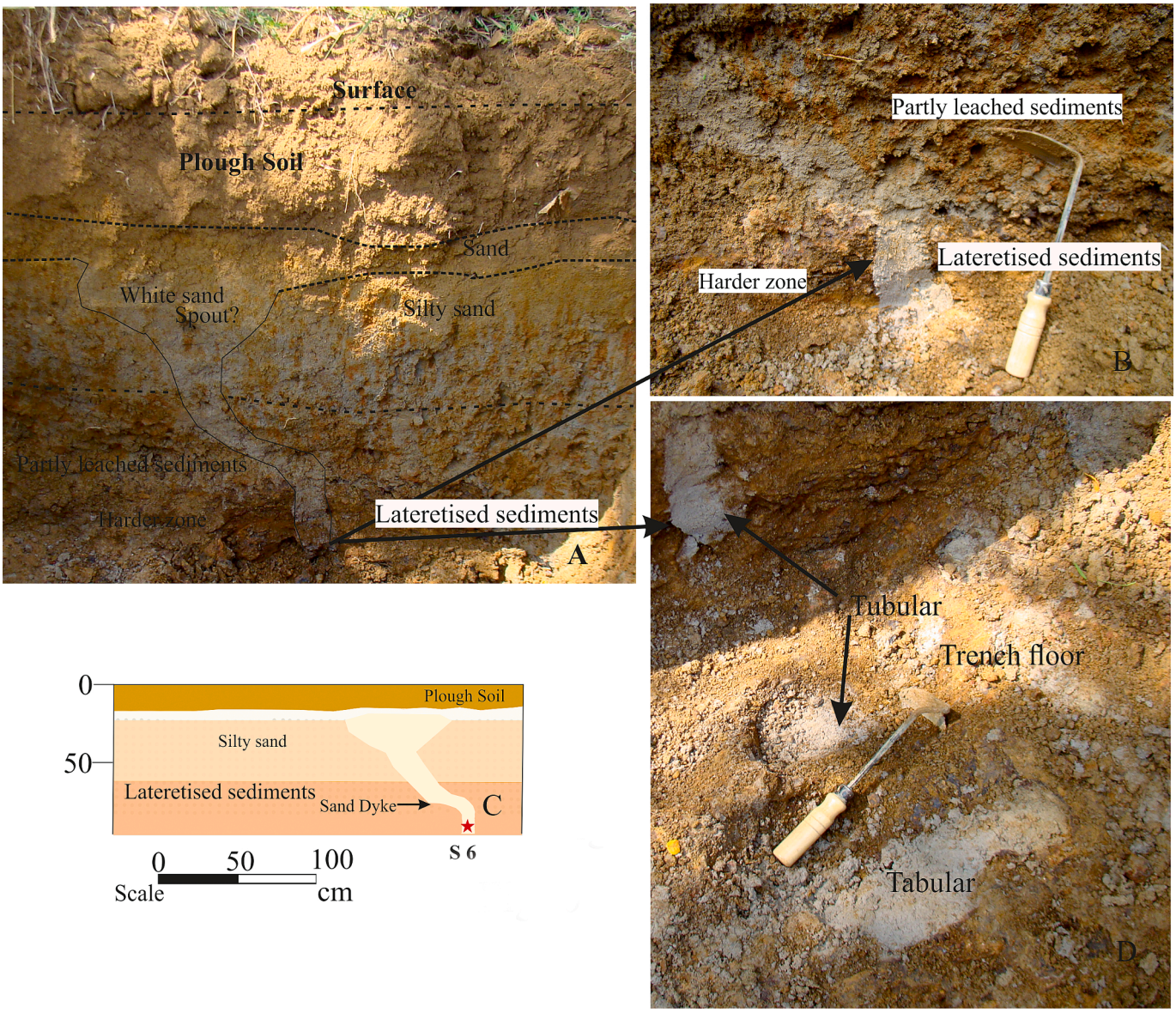

Fig. 6. Observations from Site 3. A 1-m-deep trench at Site 3 showing the liquefaction feature. A. View of the western face of the trench exposing 8-cm-thick sand dike intruding into upper units B. Closeup of sand dike C. Sketch showing lithology as exposed in the western face and location of sample collected for grain-size analysis. D. Trench floor showing two more sand dikes adjacent to the one exposed on the wall.

4.3. Site 3 (Anakkara)

As mentioned earlier, the N-S trending segment of Kuttippala valley, connecting the channels of Kuttippala in the south and Panniyur in the north is marked by a drainage divide at Site 3 (Table1; Fig. 3). The trench is located at the ~ 1.5 km north of the Site 1, at this zone of a drainage divide. The trench exposed 15–20 cm thick topsoil and plough zone, followed by 10–12 cm-thick sandy layer (Fig. 6A, B & C). The silty sand unit showed yellowish patches indicating partial weathering (Fig. 6A). The sediment below was also partly leached/mottled and the unit below a depth of 90 cm appeared partly indurated. The trench exposed an 8-cm-thick sand dike (Table 2) on the western wall, extending to the surface (Fig. 6B). Yellow stains were also noticed in the sandy dike material, indicative of leaching. We observed two more dikes on the floor of the trench adjacent to the wall (Fig. 6D). The cross-sectional view indicated their circular and tabular nature (~30 cm), and they also showed the effect of leaching. The sand dikes exposed in this trench are the thickest ones observed in this valley.

At Site 3 (Fig. 3), the sedimentation after the liquefaction event appeared negligible. The lateritisation zone is thickest at this site and can be attributed to the fact that the area remained a drainage divide even at the time of liquefaction. Stains of leaching observed in the white sand confirm that the extruded unit was possibly exposed to weathering for a long time without burial.

4.4. Site 4 (Chalissery –west)

With several tributaries joining the Chalissery valley, it forms a larger drainage area among the three studied (Table 1; Fig. 3). The main trunk of this channel trends in an east–west direction up to the west of Chalissery, from where it takes a turn towards the southwest (Fig. 3). We were not able to explore the subsurface lithology of this segment due to the very shallow water table. The westernmost part of this E-W segment was explored at several locations. At Site 4 (Fig. 3), a 2.1- m-deep-trench showed a 20 cm thick plough zone followed by a band of 30 cm of sandy soil (Fig. 7A, B & C). This unit is underlined by a 90-cm-thick clay intercalated with laterite nodules (Fig. 7B) and followed by silty sand clay up to 2.1 m depth. The sample collected from a depth of 260 cm

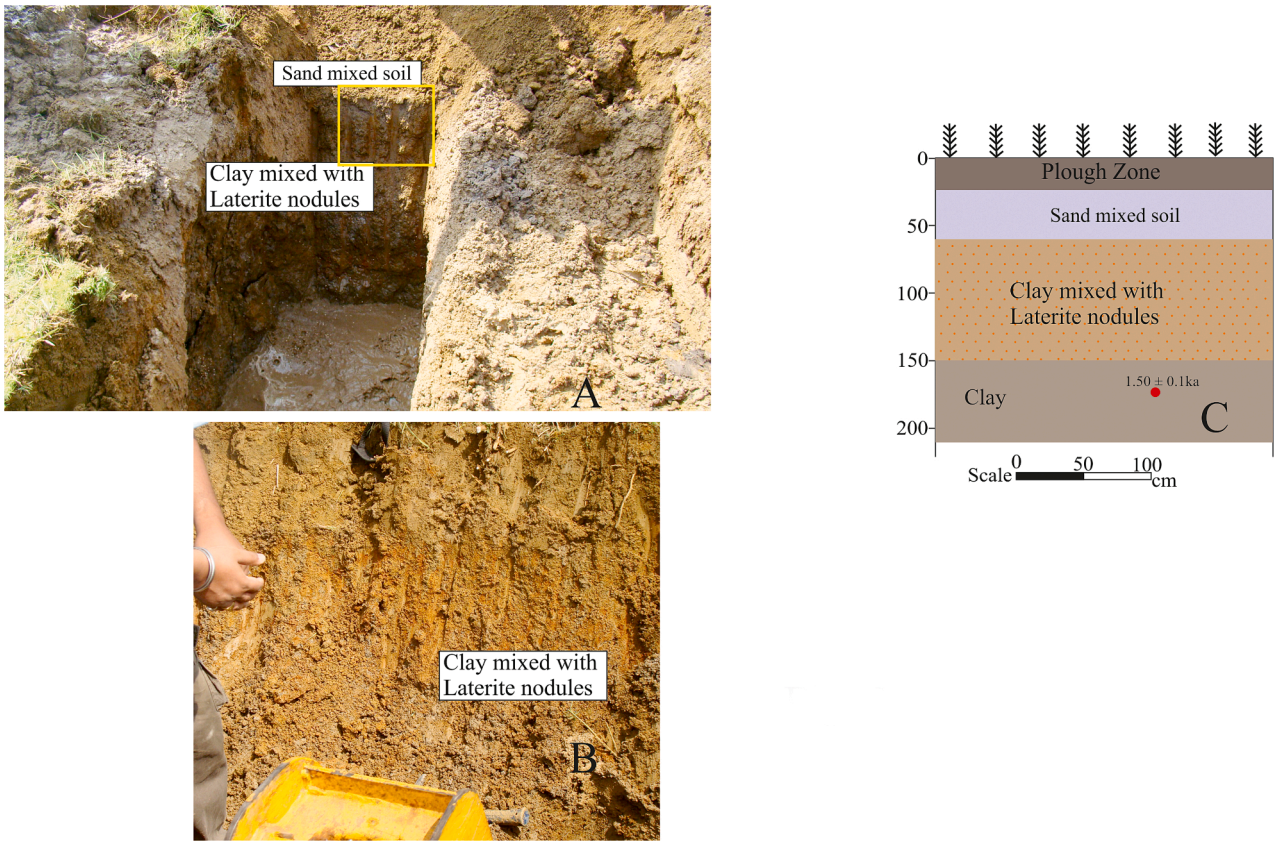

Fig. 7. Observations from Site 4. A. View of the 2.7-m-deep trench excavated at Site 4. B. Closeup of the trench wall showing different litho-units. C. Sketch showing lithology and sample location for OSL dating.

indicates an OSL date of 1.5 ± 0.1 ka (Table 4; Fig. 7C). The event that initiated the mixing of laterite nodules with clay must have happened sometime after 1.5 ± 0.1 ka.

4.5. Site 5 (Chalissery –east)

A 2.4-m-deep trench at Site 5 (east of Chalissery), where the channel maintains an east–west trend further upstream (Table 1; Fig. 3), exposed ~ 20 cm of plough zone followed by a unit of clay intercalated with laterite nodules (Fig. 8A, B & C). The 1.4-m-thick sticky clay observed below has been dated 4.5 ± 0.3 ka (Table 4; Fig. 8C). The trench bottomed on the latertitised sediments.

4.6. Site 6 (Alikkara)

Further upstream from Chalisseri, near Alikkara (Table 1; Fig. 3), in a local small pond on the southern bank of the E-W trending valley (Site 6), discordant sand intrusions were visible within the lateritised sedimentary layer, observed close to the surface (Fig. 9A, & B). The features ended up in a sandy horizon, which was overlain by a silty sand unit. The upper level was disturbed due to human activities. To confirm these features, a fresh excavation was attempted further into the valley. This trench exposed sand layers at 60 cm depth (Fig. 9C & D), overlain by a ~ 45 cm thick silty sand and ~ 20 cm plough zone. On the eastern side a flat-lens-shaped sand unit was observed (Fig. 9D). The trench also exposed two funnel-shaped sand bodies that can be characterized as surface continuity of sand dikes (Fig. 9E). The silty sand units showed an erosional contact with the bottom unit. The funnel-shaped sand unit and the lens-shaped unit were dated as 2.5 ± 0.1 ka and 0.8 ± 0.02 ka respectively (Table 4).

The observations from Site 6 suggest that the liquefaction had occurred within a layer below the zone of partially lateritised sediments. The liquefied sand penetrated the overlying sediments to reach the surface. Closely spaced intrusions are indicative of the severity of the shaking that induced the phenomena. The liquefied and extruded sediments (sand), however, do not show any signs of leaching. These trenches thus provide clues hinting at liquefaction at this location that occurred as a post-lateritisation episode.

4.7. Site 7 (Thirumittacode)

At the eastern end of the east–west trending Chalisseri Valley, close to the basin boundary of the Bharathapuzha River (Table 1; Fig. 3), we made another trench (Fig. 10), where a semicircular subsidiary valley appeared detached from the main valley (Site 7). As indicated in the satellite imagery, water from this location might be flowing either north or west (Fig. 3). The ~ 3 m-wide trench exposed a 10–12-cm thick plough zone at the top, underlain by a ~ 35-cm-thick sandy silt layer (Fig. 10A, B, C &D). A ~ 22 cm-thick sandy horizon was observed below the sandy silt. Below the sandy horizon, silty sand units of varying texture extended up to the bottom of the trench. Immediately below the sandy horizon a ~ 35 cm-thick layer of silty clay unit was observed, that showed yellow tinges, and was underlain by a light/white coloured silty sand unit (40 cm thick), followed by a ~ 1.5 m thick mottled silty sand at the bottom. The trench exposed a ~ 3.3 cm thick curvilinear sand dike (Table 2; Fig. 10B), which exhibited a minor sill formation that branched upward at about below 2.5 m depth (Fig. 10C). The top sandy silty and the bottom silty sand were layer were dated 2.00 ± 0.1 ka 2.5 ± 0.2 ka, respectively (Table 4; Fig. 10C).

The observations from this site suggest that the liquefaction had impacted a layer below the zone of thick silty sand. The liquefied sand appears to have penetrated the overlying sediments to reach the surface during the event. Although the sand observed in the dike below 1 m depth did not show any leaching effect, it exhibited yellowish tinges

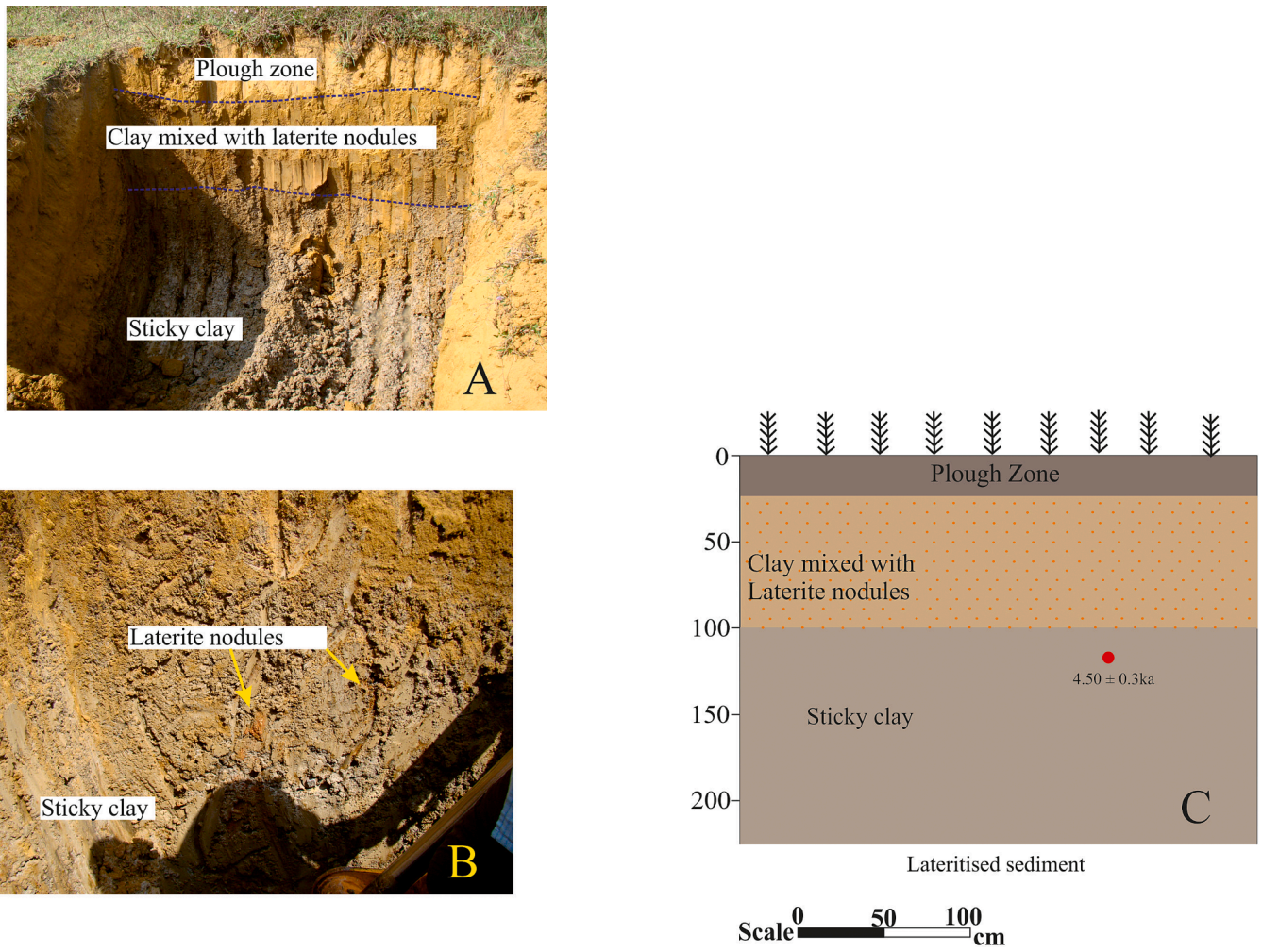

Fig. 8. Observations from Site 5. A. View of the 2.7-m-deep trench excavated at Site 5 (east of Chalissery). B. Closeup of trench wall the sandy silt showing different lithounits. C. Sketch showing lithology and sample location for OSL dating.

where it merged with the sandy horizon. Since the trench location is located close to the drainage divide, the process leading to sedimentation after the liquefaction event (sand extrusion) appears to have been very weak.

4.8. Site 8 (Perumpilavu)

As the trenches are located close to the Viyyam Kayal (estuary) are amenable to water logging resulting in very shallow water table conditions, we focused our studies a little away, along an NW-SE trending valley near Perumpilavu (Table 1; Fig. 3). The initial observation along this NW-SE channel was made from a section (Site 8) at Perumpilavu (Fig. 11), located on the western side of the Perumpilavu-Koottanad road (Fig. 3). A 2.5-m-thick layer of lateritised sediment is exposed above the water level (Fig. 11A & B) and was covered by dumped soil (up to ~ 1.2 m thick). The layering within the sedimentary units was visible in the section. Thick tabular sand dikes were exposed on the southern and eastern walls of the square-shaped well (Fig. 11A, B, C & D), which were sourced from a huge sill-like sand body occurring at a depth of 1–1.4 m from the zone of lateritised sediments. The liquefied sediments have been emplaced along the bedding planes.

At the time of our studies, the south and east walls were freshly cut (Fig. 11A, B, C & D) whereas the north and south walls aligned with the extended part of an old circular well (Fig. 11E & F). The sill was present in all the walls. The dikes were 12–25-cm-thick, and they reached the surface of the weathered layers (Fig. 11A, B, C & D). A vertical offset was observed at the level of the lateritised formation on the southern wall, most likely formed due to the fracturing/deformation or after the ground shaking /liquefaction event (Fig. 11A & B). An analogous offset was noted on the western side of the northern wall (Fig. 11E). The vertical openings in the north and west walls (observed below the retaining wall) may represent the paths of sand intrusion (dikes), which had been eroded (Fig. 11E &F). The white sand within the dike is dated 7.0 ± 1.1 ka, which occurs below the lateritised sediments, indicating that the overlying sediments could be younger than 7000 years (Table 4). The lack of leaching within liquified sediments (dikes and sills) suggests no initiation of leaching after the event of liquefaction.

4.9. Site 9 (Perumpilavu)

On the eastern side of the road at Site 9 (Table1; Fig. 3), a 1-m-deep trench exposed lateritised sediments and a sandy layer, below the plough zone (Fig. 12A & B). Grain size analyses indicate that these sand units could be of the same origin (Fig. 16), as the one observed on the well section as shown in Figure 11. This sand layer unit was dated 0.7 ± 0.08 ka (Table 4), which may represent the time of liquefaction event.

4.10. Site 10 (Perumpilavu)

To confirm the above referenced sandy unit's stratigraphic relationship, we made a couple of trenches further east of this location (Table1; Fig. 3) towards the middle of the valley (Fig. 13A, B, C & D).

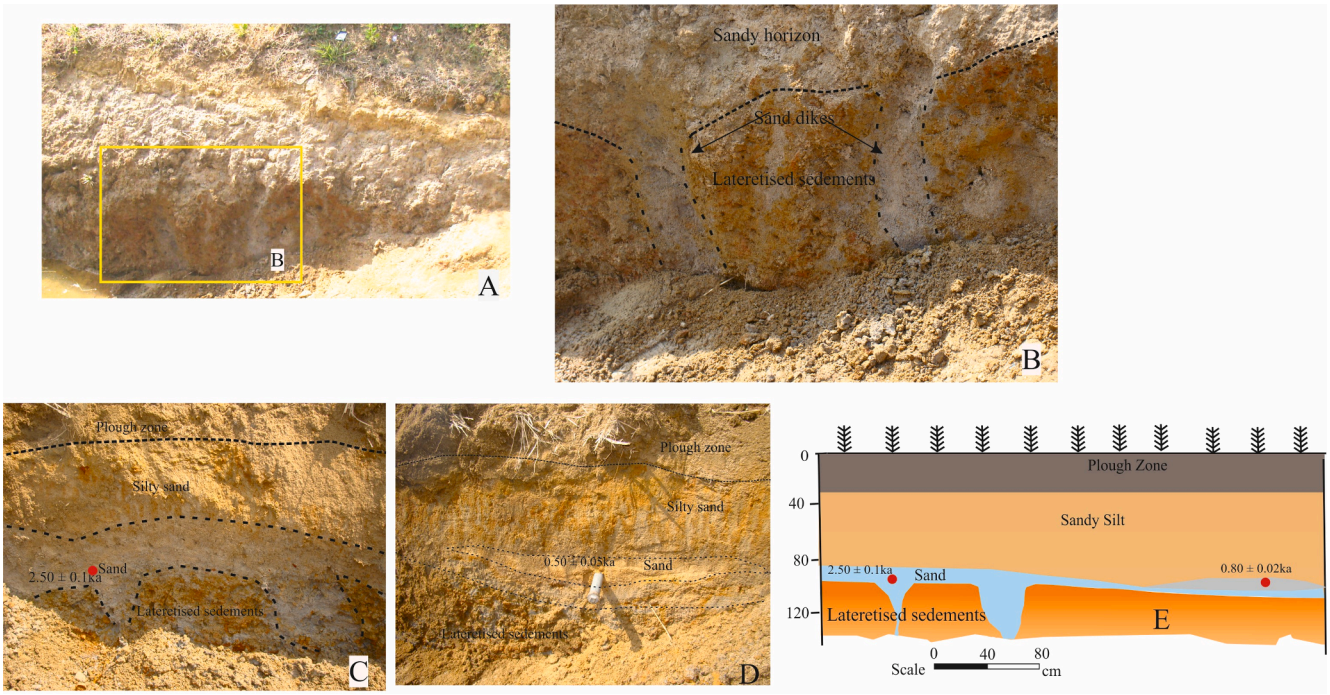

Fig. 9. Observations from Site 6. A. Artificial cutting for a local pond showing sand dikes. B. Closeup view of the dikes. C. ~ 1.5 m deep trench excavated near the earlier location shows sand dikes and emplacement of sand. D. The flat-lens-shaped sand unit observed in the eastern side side of the trench. E. Sketch showing lithology of the trench wall and two dikes. Sample locations for OSL dating are also marked.

These trenches exposed (Site 10) three litho-units below the plough zone. Although these trenches exposed sandy units having a funnel-shaped downward continuity above the zone of lateritised sediments the excavations could not be extended below 1.2 m due to the gushing of water and wall collapse (Fig. 13A & B). A layer of yellowish silty sand (partly leached) with varying thickness was observed above this sandy unit. The sediment collected from the funnel-shaped structure at Site 10 provided the OSL age 3.1 ± 0.7 ka BP (Table 4).

4.11. Site 11 (Perumpilavu)

A third excavation (Site 11) in the same valley reached 2.2 m depth and exposed ~ 1 m of lateritised layer at the bottom part of the trench (Fig. 13C). This section exposed dikes containing sand units that spread over the surface of the lateritised formation (Fig. 13C & D) – comparable to the features recorded from the well-section, as discussed earlier (Fig. 11). Silty sand unit of ~ 60 cm thick above these units was capped by 15–20 cm of plough zone (Fig. 13C & D). The sediment collected from the funnel-shaped structure provided an OSL date 4.4 ± 0.8 ka, indicative of the age of the source sediment (Table 4).

The observations from Sites 8, 9 &10 suggest that the liquefaction had occurred in a layer below the lateritised formation and emplaced through it to reach the surface. The observation from the well suggests extrusion of huge quantities of liquefied sediments, as also evident in the nearby trench. This extruded sand unit was dated 0.7 ± 0.08 ka, representing the timing of liquefaction event that must have occurred ~ 700 years ago, that was subsequently buried. The nearby shallow trenches in the valley suggest another liquefaction occurred at the end of the lateritisation. A semi-leached silty sand is observed above the liquefied sediment and the age of the liquefied unit (3.1 ± 0.7 & 4.4 ± 0.8 ka) is suggestive of the fact that the event observed in shallow trenches could be older than the one observed in the well (Fig. 13).

4.12. Site 12 (Kotol)

On the downstream side near Kotol, the Chalisseri Channel is joined by an EW-trending tributary. The trench at Kotol (Site 12) was located further south where this E-W trending tributary is joined by another NNW-SSE trending smaller tributary (Table1; Fig. 3). The trench exposed a 40 cm-thick plough zone at the top (Fig. 14A &C). A ~ 70 cm thick dark silty clay with reddish patches occurring below the plough zone. It was underlain by a ~ 60 cm thick layer of yellow sticky clay. A peat bed of ~ 60 cm occurred below the yellowish sticky clay (Fig. 14A &B), underlain by a layer of coarse sand. This location is about 11 km from the coast. Such stratigraphically positioned peat beds were observed in the north and south of this area and their formation dates fall between 8 and 5 ka (Rajendran et al., 1989; Shajan, 1998; Alappat et al., 2021). The presence of a peat bed and sandy horizon below conforms to the interpretation that the channel was active around ~ 5 to 8 ka.

4.13. Site 13 (Kanjirakkod)

A north–south trending valley occurred close to the basin divide of the Bharathapuzha River near Kanjirakkod (Fig. 3). An artificial pond was excavated in the middle of the valley at Site 13 for cultivation (Table 1; inset of Fig. 3). The section exposed indurated lateritised formation covered by a thin (20 cm) layer of soil (Fig. 3B). A thinly developed soil was observed above the lateritised formation and the area likely remained above the level of the active depositional process until recent times. The open fractures within lateritised formation are indicative of the fact that, fractures were formed after the termination of the weathering process.

4.14. Site 14 (Kuttanadu)

North of the basin boundary near Kuttanadu, indurated lateritised part of sediments overlayered by a thin apron of soil were exposed in an artificial pond at Site 14 (Table1; Fig. 3), built at the southern end of the north-trending valley (Fig. 15A). A north dipping fracture was visible on the southern wall at this site (Fig. 15B). The hanging wall side of the fracture is relatively stable and more intact, whereas the footwall side

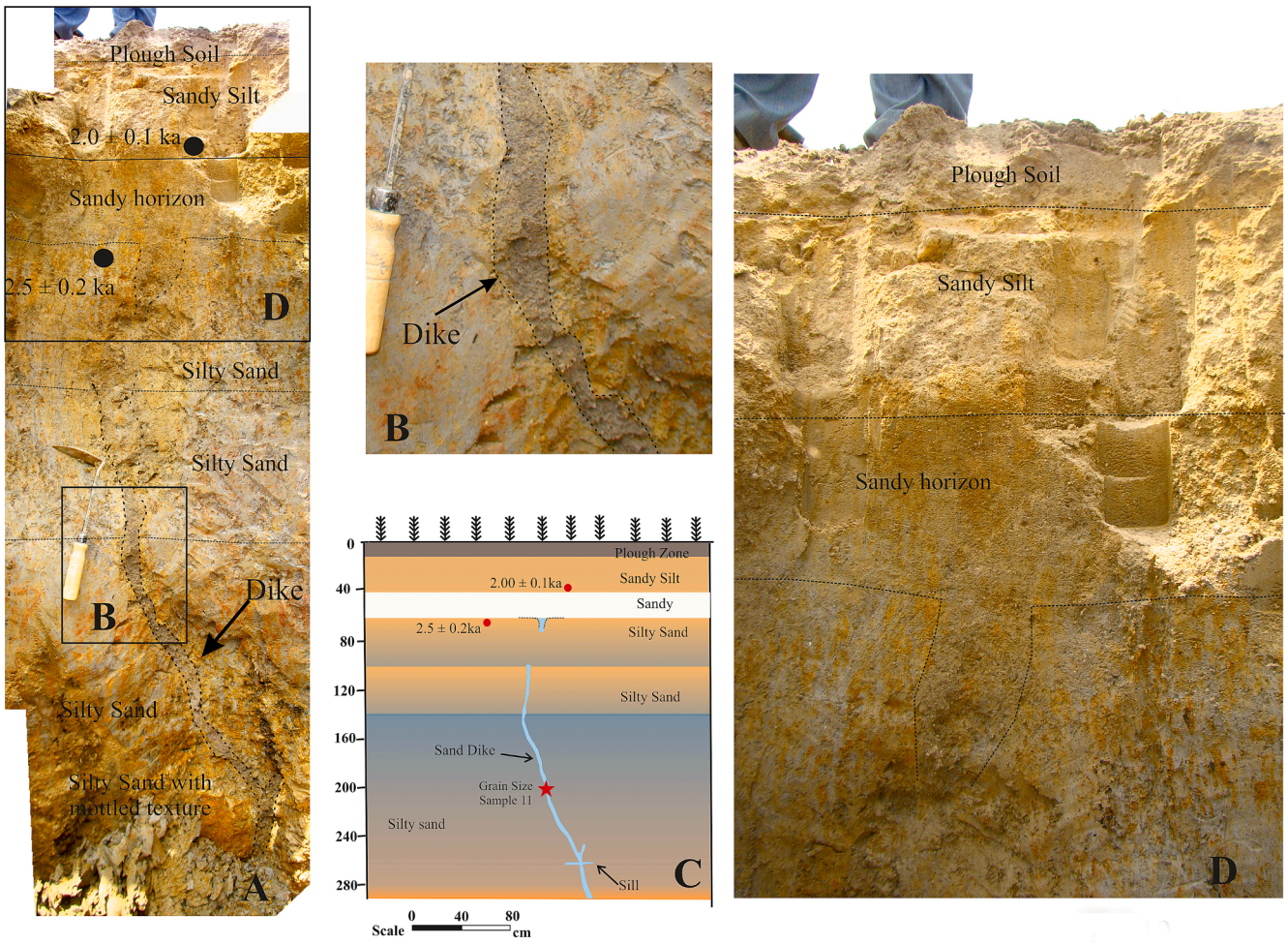

Fig. 10. Observations from Site 7. A. The 3-m-deep trench shows different lithounits and sand dikes: The rectangles are the portions zoomed in B and D. B. Closeup of sand dike cutting across silty sand unit. C. Sketch showing lithology of the trench wall decifering the trace of the sand dike. D. Closeup view of the upper portion of the trench showing the top end of dike and overlying sedimentary units.

shows further fracturing with numerous smaller fractures reaching up to the soil cover. Further 2 m southeast on the footwall side, a prominent vertical fracture was observed, and some hard lateritic pieces appeared to have been trapped in the open fracture. We could also observe some gentle buckling in the zone between these two fractures (Fig. 15C). As in the previous section, the thin layer of soil above the lateritised formation may indicate that the area remained above the depositional process until recently and the fractures developed after the lateritisation process ceased.

4.15. Site 15 (Velladikunnu)

Further east within the boundary of the Bharathapuzha basin (Table 1; Fig. 3), indurated lateritised sedimentary sections were observed in an open well (Site 15) with south-dipping interconnecting fractures (Fig. 15D). The northernmost fracture was filled with lateritised sediments and hard lateritic pieces. There was a zone of highly fragmented hard lateritised sediments observed where two south dipping fractures were merged and were overlain by a cavity and the hard part of lateritised formation in this zone appears to have been structurally buckled (Fig. 15D). The nature of fractures indicate that they developed after the lateritisation process ceased.

5. Discussion

The present study is focused on understanding the shallow stratigraphy in the southern side of the Bharathapuzha River. The shallow-level trench sections indicate that despite the proximity of the study area to the coastal wetlands, the valleys investigated here are indeed paths for the earlier river/drainage, as evident from the presence of riverine sediment. Trenches made close to coastal wetlands (Sites 4 & 5) show thick clay deposition with dates ranging from 4.5 ka to 1.5 ka BP (Figs. 7 & 8). Farther from the coast (>10 km) the trenches show predominantly of sandy sediments. Peat formation was part of a significant geological event observed in the area. A deep trench at Kotol exposed peat bed which is comparable to the one formed between 5–6 ka BP as reported by Rajendran et al. (1989), not very far from the current study area.

The post-Pleistocene lateritisation of the younger sediments in the southern part of Peninsular India was first reported by Mallikarjuna et al. (1980). The present observations further confirm the laterization as a continuous process under favourable climatic conditions. The trench sections showed a spell of lateritisation/leaching younger than 7 ka, BP. For example, in an open well in Perumpilavu (Site 8) up to 3-m-thick lateritised sediment is observed (Fig. 11). Leaching effect was identified by iron staining even in younger sediments (~2 ka) at Site 2 (Fig. 5). At Site 3 and Site 6, the topmost sediments (sandy silt), which could be younger than 0.8 ka BP, also showed ferruginous trails (Fig. 9). The liquified sand observed in the trenches at Sites 3,6,7,8,9,10 &11 have their source located below the lateritised sedimentary unit.

Close to the basin boundary of the Bharathapuza River, fracturing was observed in lateritised sediments. This should be evaluated in

combination with the reports of mid-Holocene land-sea interactions and peat bed formation identified adjacent to this area (Alappat et al., 2021). There is a historically reported flood event that damaged and abandoned a seaport at Kodungallore located north of Kochi and the emergence of the land at the coastal part of Kochi in the year CE1341(e.g., Newbold 1846; Rajendran et al, 2009). In the present study, we noted a mixing of laterite grains with clay units at two trenches in Sites 4 & 5. Since these locations are within the wetland, the mixing could have happened due to the flushing out of laterite nodules from nearby laterite terrain during the CE 1341 flood.

5.1. *Mechanism of formation of liquefaction features*

Liquefaction is generated when the sediment loses its strength due to the cyclic shear stress generated by an earthquake. The liquefied sand is injected in the overlying sequence through weak zones in the cap layer and this injection path gets preserved as sand dikes. The three ground failure mechanisms observed during the development of dikes are (1) hydraulic fracturing (2) lateral spreading and (3) surface oscillation (Obermeier 1996). The present study considered all the known scenarios for the origin of sedimentary features discussed here, including dewatering due to rapid sedimentation and compaction is one of the more common causes of *syn*-depositional, non-seismic, liquefaction features; artesian conditions as suggested by Lowe (1975); Owen (1987) and

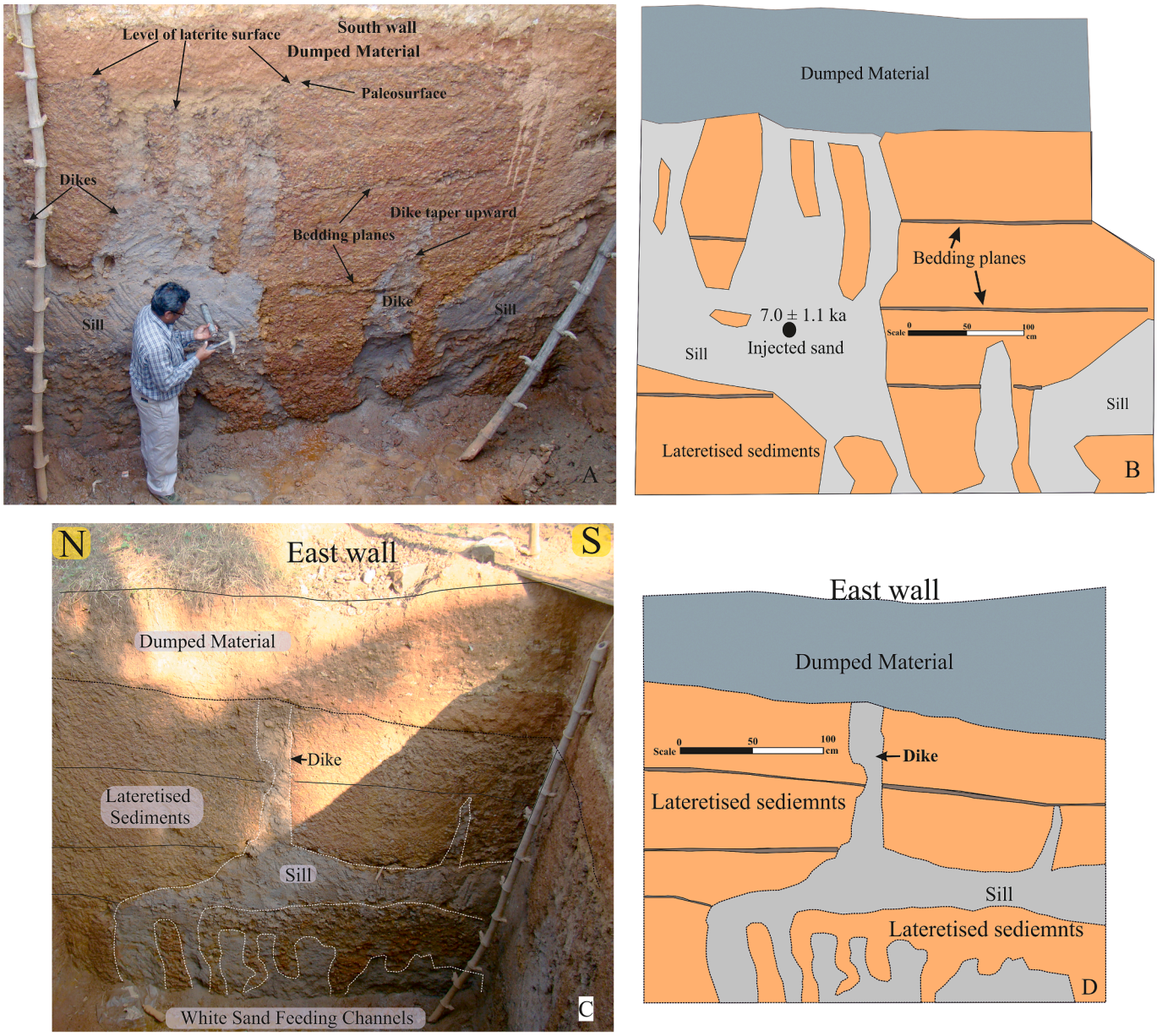

Fig. 11. Observations from a square-shaped well at Site 8. A. Liquefaction features observed in the southern wall of the well. The original layering of the sediments is preserved in the lateritised sediments that host the empalced sediments. Note that the sand dike originates from a visible sand sill. The multiple dikes extending up to the surface are also associated with the change in the level of lateritised sediments. B. The sketch of the southern wall of the well showing the thickness of the injected sand, bedding planes and size of the sill. C. Sand sill and dike exposed on the east wall; note the multiple dikes observed below the sill. D. The sketch of the east wall of the well, showing thickness of the dike and sill. E. Annotated photo of the north wall of the trench, partly covered by a retaining wall. The vertical opening may indicate a dike from which the sand is eroded; the hollow zone below is an eroded potion of sill. The vertical fracture marks the offset extending to the ground level. F. Annotated photo of the north wall of the trench, partly covered by the retaining wall. Part of the uneroded sill and vertical opening in lateritisd sediments are also visible.

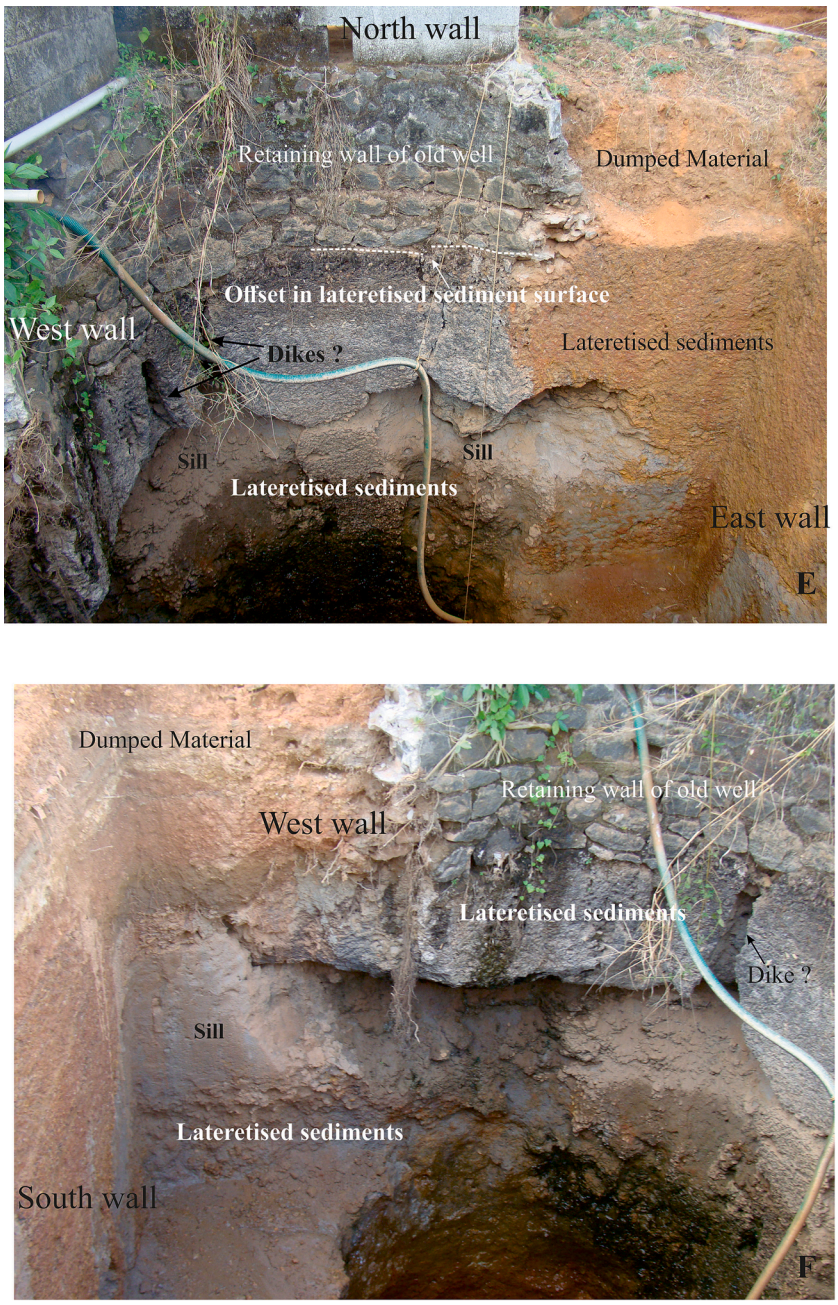

Fig. 11. (*continued*).

Holzer and Clark (1993). We have used the following criteria to identify the reported features as earthquake-induced liquefaction features we have used the following criteria. (1) sedimentary characteristics indicative of sudden, strong, upwardly-directed hydraulic force of short duration; (2) occurrence of more than one type of liquefaction feature and similar features at multiple locations; (3) occurrence in geomorphic settings where hydraulic conditions as described under the first criterion would not develop under non-seismic conditions; and (4) age data to support both contemporaneous and episodic formation of features over a large area.

In the present study, most of the dikes seem to be produced by hydraulic fracturing. In this type of failure mechanism, the fracturing of the cap typically occurs in response to the high pore-water pressure from the base of the cap. The small root holes or other natural openings, if available, will control the hydraulic fracturing (Obermeier et al., 2005). Hydraulic fracturing typically produces tabular dikes and generally parallel to one another but may also be found haphazardly in planar and sectional views, where liquefaction is severe. The observations suggest that where dikes show branching the chances of venting of liquefied sediments diminish due to effective dispersion of energy (Obermeier 1995). The occurrence of numerous sub-parallel dikes and the branching types observed in the trenches of the present study area may indicate the same effect. On the contrary, the thickness of the dike and the change in surface elevation of the pre-liquefaction surface may indicate the influence of lateral spreading in the formation of dikes.

5.2. *Event chronology*

We developed the temporal constraints from different sites to identify the earthquake event/s that caused the liquefaction and associated sediment deformation (Fig. 17). The oldest host sediments in the present study at Site 1 provided a date 10.7 ± 0.9 ka BP. Liquefaction events in

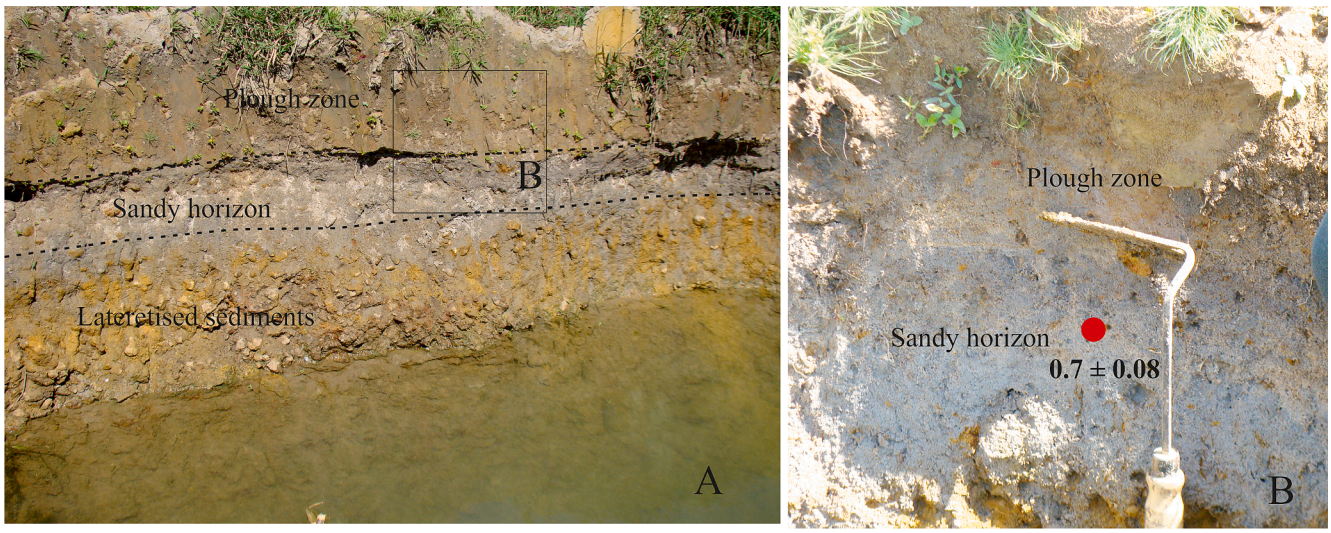

Fig. 12. Trench exposure about 50 m east of the well located at Site 9 is shown in Fig. 11. A. trench wall showing lateritised sediments, sand layer and plough zone. B. Cleaned section showing the sandy horizon resembling the dike and sill material observed in site 8.

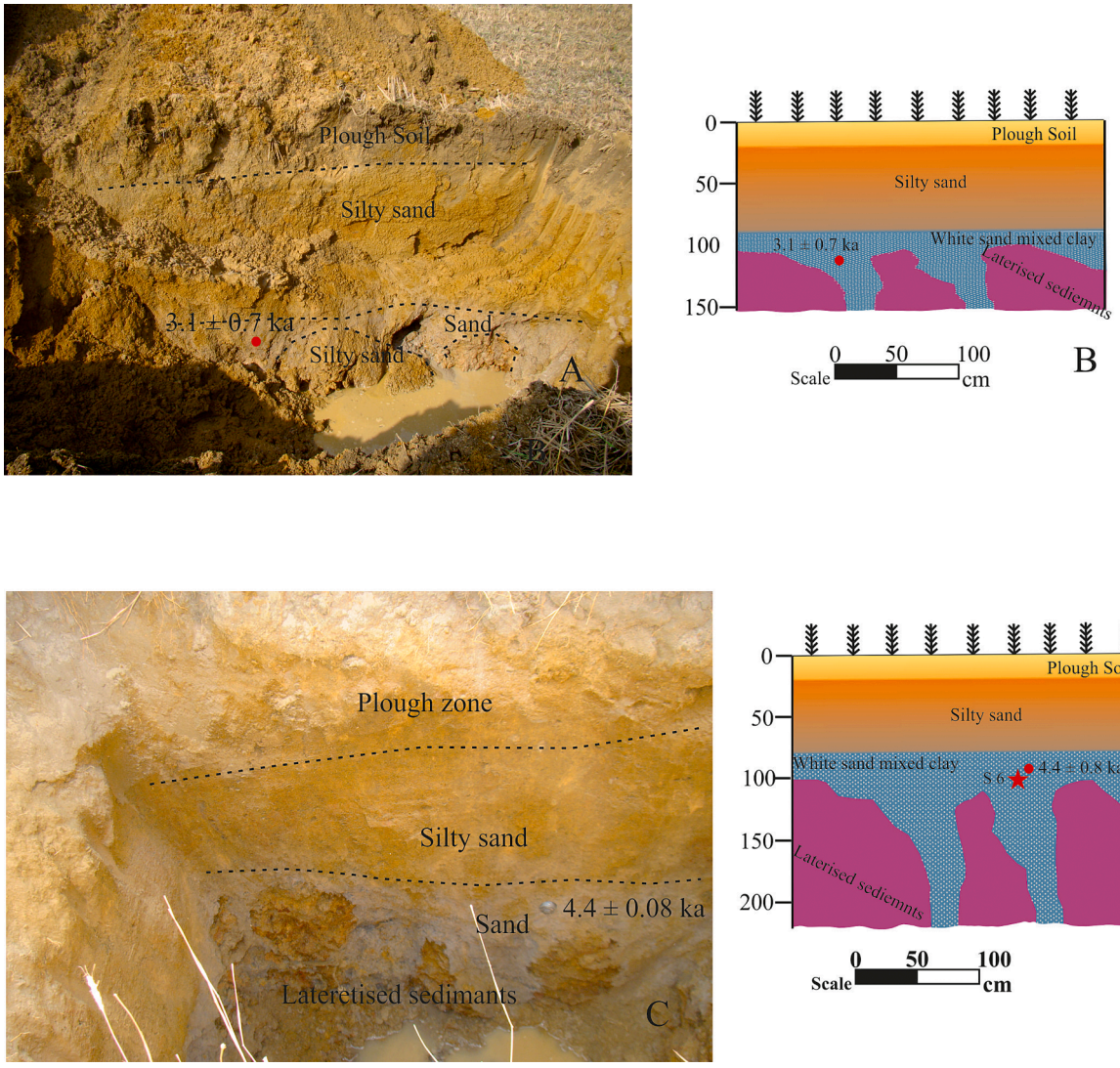

Fig. 13. Trench excavations in the middle of the valley at Sites 10 and 11. A. The trench exposure at Site 10 shows a loose sandy horizon at the bottom. The sandy units, resemble the dike and sill material observed in site 8. B. The sketch showing lithology and dikes exposed at site 10. The location for OSL dating sample is also marked C. A 2.2-m-deep trench excavated at Site 11 shows the dissected nature of lateritised sediments and unaltered sandy units resembling the dike and sill material observed in site 8. D. The sketch showing lithology and dikes exposed at site 11. The location for OSL dating sample and sample collected for grain-size analysis 'S6' are also marked.

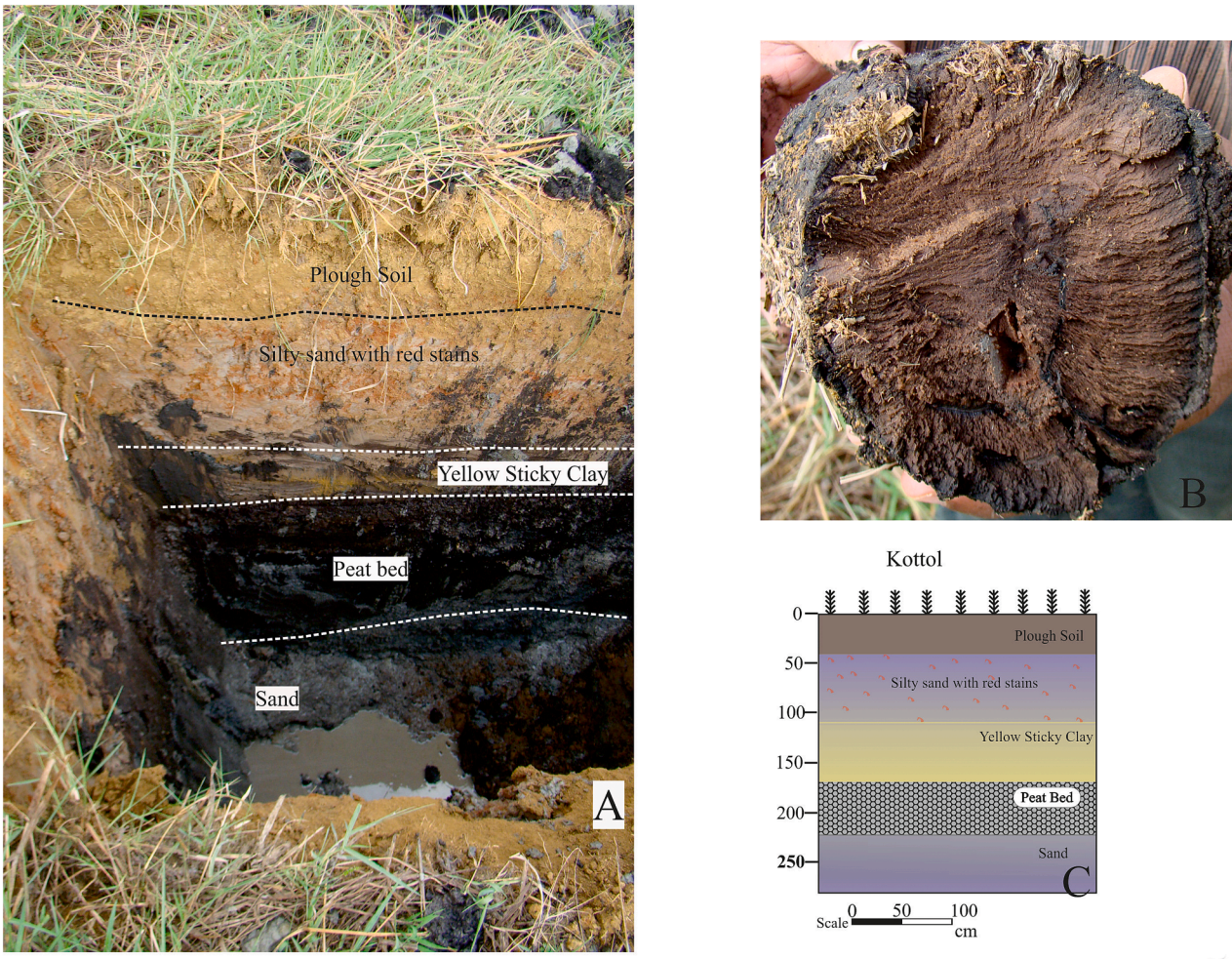

Fig. 14. Site 12. A. 3-m-deep trench excavated at Site 12 (Kotol)site exposed peat bed. Note the white sand below the peat bed. B. One of the wodden piece observed in the peat bed C.Sketch showing the litho-section of the trench.

general occurred to sandy units below the lateritised sediments. The liquefied sediments observed in the well at Perumpilavu (Site 8) further suggest the source material could be from a bed (7 ka BP) older than the interval of peat formation (~5–6 ka), whereas the other shallow trenches the source material is younger than peat bed. The nature of the sediments observed in trenches well away from the wetland suggests the leaching process (beginning of lateritisation) commenced in sediments earlier (around 2 ka BP). This suggests two different liquefaction events – an older event E-I (between 2.2–2.5 ka. BP) and a younger event E-II (0.7–0.8 ka BP). The details of the event characterization are discussed as under:

5.2.1. *Event-I (E-I)*

Event −1 has been inferred from the age constraints of the liquefaction event observed at Site 1(Fig. 5), Site 6 (Fig. 9) and Site 7 (Fig. 10) locations. Five lower bound OSL ages of samples with numbers LD1875, LD 1832, and LD3579, indicate an age of 2.5 ka BP while its upper bound is provided by the samples LD 1475, LD 1831, LD1833 with an age of 2200 ± 100 years BP. The age data implies that the liquefaction feature could have been formed between 2000 years (UB) and 2500 years (LB).

5.2.2. *Event- II (E-II)*

This event has been inferred from the age constraints of liquefaction observed at Site 6 (Fig. 9) and Site 9 (Fig. 11&12). Both these locations show an age of 0.8 ± 0.02 ka and 0.7 ± 0.08 ka for the emplaced material, indicating the event could be as young as ~ 0.78 ± 0.08 ka BP. The flood event (1341CE) at ~ 0.681 ka BP is younger than this liquefaction event. There is a second set of sand intrusion features observed at Site 1, as inferred from the textural differences of the liquefied materials (Fig. 4). We could not constrain the age of this intrusion as it terminated within the host sedimentary unit of 10.7 ± 0.9 ka BP. This simply suggests that the second liquefaction event at Site 1 postdates 10.7 ± 0.9 ka BP.

5.3. *Signatures of deformation in the indurated part of lateritised sediments*

It is reported that the Indian landmass has witnessed a lateritisation process since pre-Oligocene (Frakes and Kemp 1972). A long spell of lateritisation generally removes all original rock structures and thus makes it difficult to identify the parent rock. The continuity of the lateritisation process under favourable conditions during the post-Pleistocene period is also identified in Kerala in the sedimentary formations (Mallikarjuna et al., 1980). Our trench sections further confirm the leaching process on sediments as young as 2000 years BP. Thus, it can be suggested that the fracturing in the indurated part of lateritised sediments belongs to a young episode of deformation.

5.4. *The causative Structure/s*

As for the study area, the geologic studies conducted after the M_w 4.3

Fig. 15. Fractures present in the indurated part of lateritised formation. A. North dipping (40°) fracture observed in the indurated lateritised sediments near Kootanadu (Site 14). B. Vertical open fracture south of the inclined one that contains trapped pieces of indurated part of lateritised sediments. C. Gentle buckling observed between the vertical fracture and the inclined one. D) South dipping fractures observed in the hardened part of the lateritised sediments exposed in the well near Velladikunnu (Site 15). Note both fractures are filled with fragments of hardened parts of lateritised sediments.

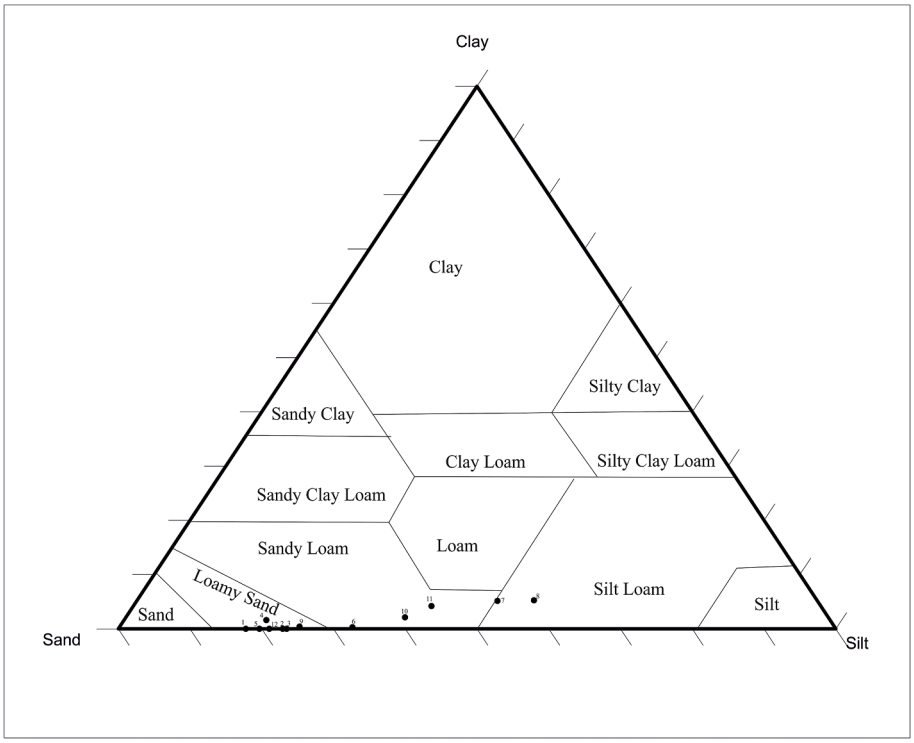

Fig. 16. Sediment samples plotted in Trilinear Diagram. Refer to Table 1 for locations.

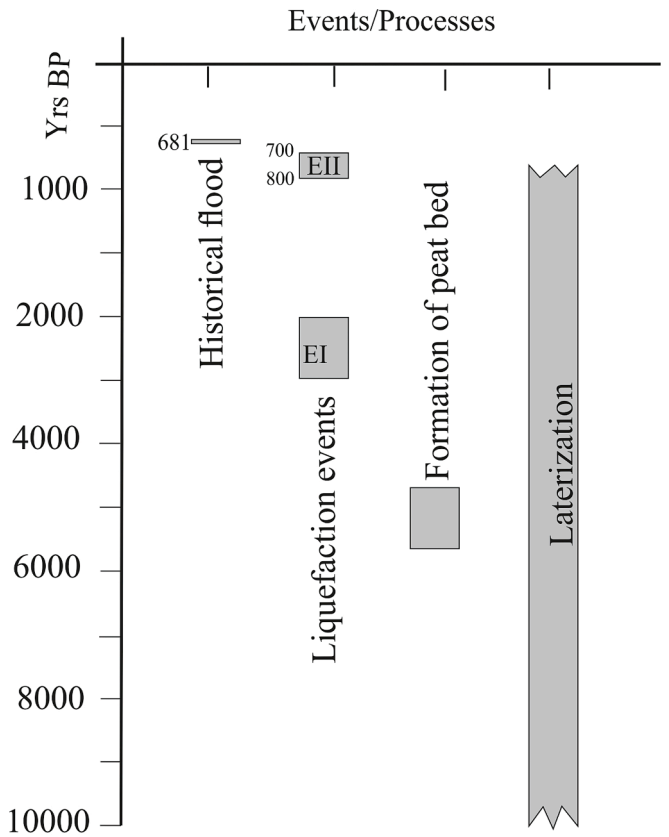

Fig. 17. Chronological sequence of various events identified in the present study.

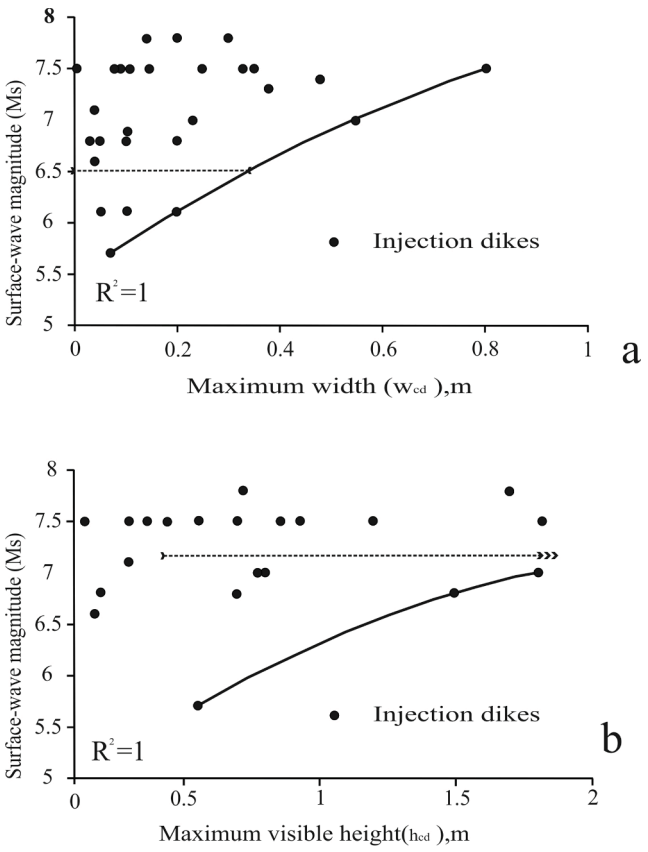

Fig. 18. Bounding curves of the earthquake magnitude vs. the dike parameters derived by Lunia and Gladkov (2015): a) maximum width; b) maximum visible height; the dotted lines represent the output derived from the present study.

Wadakkancheri earthquake of 1994 identified the causative structure and named it the Desamangalam fault (Supplimentary material), which is also interpreted to have influenced the course of the major river in the region, the Bharathapuzha River (John and Rajendran 2008). Detailed field and laboratory studies of the surface exposure of the fault identified four episodic movements on this fault and it is indicative of faulting at shallow depth (John and Rajendran 2009).

John and Rajendran (2009) further analyzed this fault, having a length of > 30 km and suggested that the fault has the potential to generate M ≥ 6.0 earthquakes. The dislocation of the fault is measured as ~ 2 m from the offset markers and is also supported by the thickness gained by the gouge zone. Since four episodes of activity are recorded on this fault, the authors suggest a mean displacement of ~ 50 cm could have occurred for each faulting episode. Available data from continental faults (Sibson, 1989; Wells and Coppersmith, 1994; Rajendran et al., 1996) show that a movement of 50 cm along the fault could be associated with an earthquake of magnitude M ≥ 6.0. Further it is found that loose gouge from this site has yielded an age of 430 ± 43 ka for the last major faulting event (ESR dating), that reset signals stored in inherited defect centres of the quartz grains from natural radiation (Rao et al., 2002). Though the date of the fault gouge is related to exhumed exposure of the fault zone, this data suggests that this fault may be seismogenic, judging by SCR standards of earthquake recurrence where probably moderate earthquakes may recur in tens of thousands of years or hundreds of thousands of years at one source (e.g. Johnston and Kanter, 1990).

5.5. *Possible size of the event*

The present study found evidence of paleoliquefaction, spread over an area of about 100 sq km, which is a surprise discovery from the southern part of peninsular India (Fig. 3). The evidence indicates that the sand injection cut through more than 3 m of overburden with a maximum width of ~ 30 cm (Site 7). There are two more locations (Site 1 and Site 7) where the dike heights exceed 2 m (Table 2). These three locations are located on the periphery of the liquefaction zone identified in the area. That may indicate that the liquefaction event might extend beyond the present study area. Based on the height and width of the dikes from global data, Lunina and Gladkov (2015) introduced an empirical relation with surface wave magnitude. Plotting our data using this relation, indicates that the dimensions of the liquefaction features in the present study area align with magnitude range > 6.5 (Fig. 18a &b).

To estimate the intensity of the earthquake that triggered liquefaction, we use here the empirical relationship of Galli and Ferreli (1995) Eq. (1):

$$Io = e^{2.04+0.003(d)} \quad (1)$$

Where; Io = Intensity (MCS) and d = epicentral distance (km). Considering the epicentral distance as 11 km which is the distance from the Desamangalam fault to the farthest liquefaction structure observed at Site 8, the maximum minimum intensity (Io) triggered by the causative earthquake is estimated as 7.95 (Io = 7.95).

To calculate the bounding/lowest intensity of the earthquake triggering the observed liquefaction, we use here the empirical relationship of Galli (2000) Eq. (2) to determine:

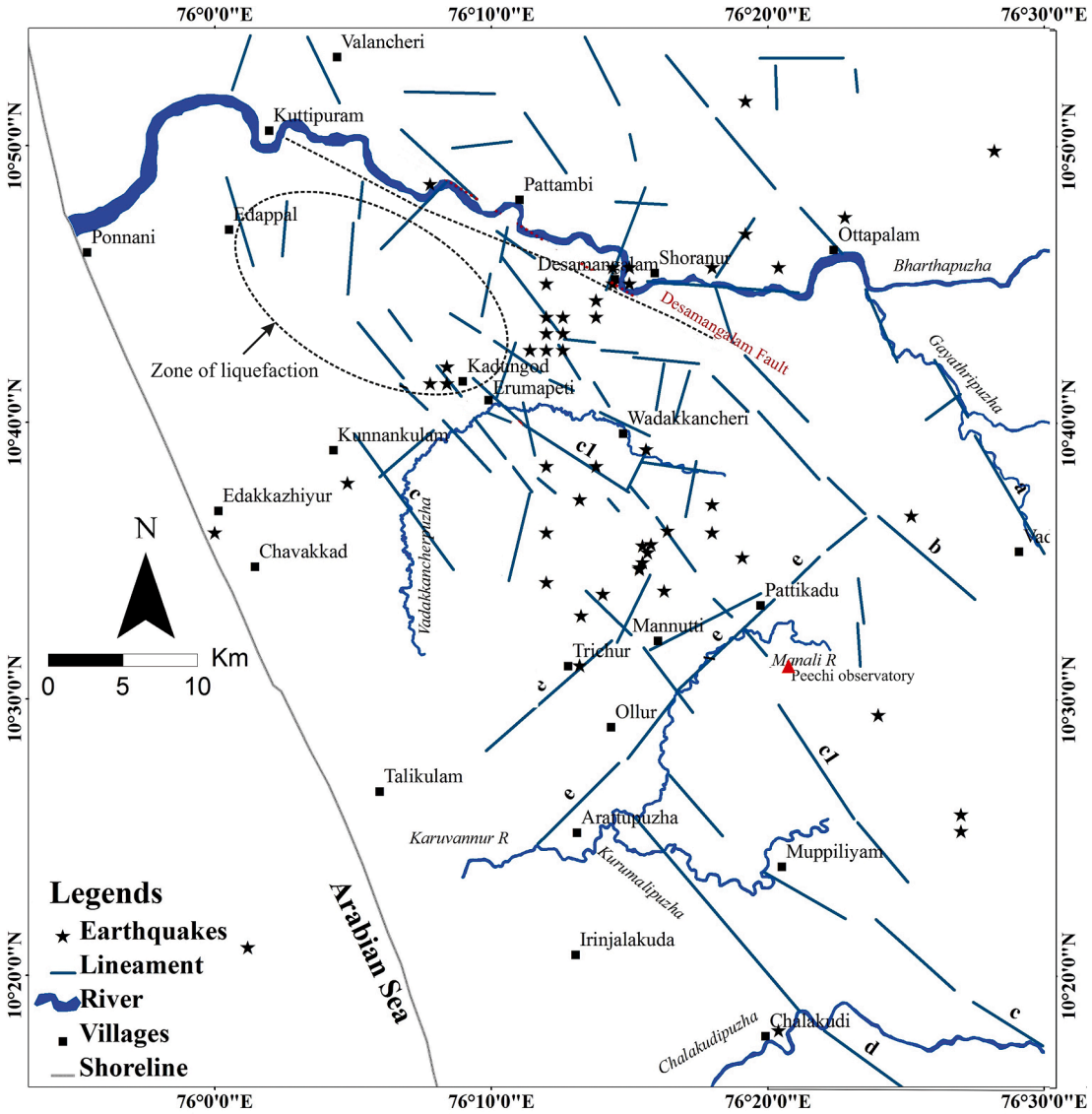

Fig. 19. Location of low-level earthquakes within the study area (until 2015: Singh et al 2016b). The zone of liquefaction is marked by an ellipse. The filled triangle indicates the location of the Seismic Observatory at Peechi. The lineaments are adopted from Singh et al. (2016b) and those numbered C and C1 are considered as extended parts of the Periyar fault.

$$Io = 1.6 + 4.3 \text{ Log } (R_e) \quad (2)$$

Where; Io = Intensity (MCS) and R_e = epicentral distance (km). Considering the epicentral distance as 11 km which is the distance from the Desamangalam fault to the farthest liquefaction structure observed at Site 8, the minimum intensity (Io) triggered by the causative earthquake is estimated as 6.08 (Io = 6.08).

We have also estimated the Environmental Seismic Intensity (ESI-2007) scale (Michetti et al., 2015; Serva et al., 2016) for the present observations and on the total area affected. Rare cases of liquefaction for intensity VII (ESI-2007) occur in areas most prone to the phenomenon. Our data suggest an intense liquefaction phenomenon within > 100 km^2 area and is comparable with an intensity of VIII on ESI-2007 scale, along with localized lateral spreading. This value closely matches the intensity calculated from eq1 (7.95) of Galli and Ferreli (1995) and is two levels higher than the one calculated by Galli (2000).

Naik et al. (2020) unified the intensity observations of the 1819 Allah Bund ($M_w \approx 8.0$) and 2001 Bhuj (M_w 7.7) earthquakes. Though there are disputes about the magnitude of the 1819 Allah Bund earthquake (Rajendran and Rajendran 2020; Sunilkumar et al., 2024), the epicentral intensity (ESI-2007 scale) estimated is the same for both earthquakes (Naik et al, 2020).

We have also estimated the magnitude of causative earthquake(s) calculation based on empirical relations of Ambraseys and Jackson, 1998 Eq. (3) Gutenberg and Richter, (1956) Eq. (4) and Galli (2000) Eq. (5).

$$M = -1.74 + 0.66 \times I + 0.0015 \times R + 2.26 \times \log R \quad (3)$$

Where, M = Magnitude, I = Epicentral intensity, R = hypocentral distance.

$$M = 1 + 2I_0/3 \quad (4)$$

Where, M = Magnitude, Io = Epicentral intensity.

Using the empirical relations of Ambraseys and Jackson (1998), the magnitude of the causative earthquake is estimated to be 5.9 M_w on considering $I = 7.95$ (obtained from eq (1) and $R = 11$ km.

Using the empirical relations of Gutenberg and Richter (1956) the

magnitude of the causative earthquake is estimated to be M_w 6.3 considering $I = 7.93$.

As per Galli (2000) bounding/lowest magnitude (M_s) of the earthquake capable of triggering the liquefaction is calculated based on the following empirical formula (Eq. (5).

$$M_s = 1.0 + 3.0 \text{ Log } (R_e) \quad (5)$$

The result shows that the minimum magnitude responsible for triggering liquefaction is 4.2. indicates In an earlier study (Green and Bomme (2019), it is concluded that the minimum moment magnitude required is 4.5 that can trigger liquefaction in extremely susceptible soil deposits. Here in the present case, the liquefaction is widespread and thus this relation (eq. (5) may not be applicable.

According to Ambraseys (1988), there could be inaccuracies in the estimation of magnitude range between 0.25 and 0.5 for recorded events and can be of the same magnitude for historical or pre-instrumental earthquakes. Historic earthquakes that occurred in intra plate settings in Australia (M_s 6.5 and 6.8; Collins et al 2004) and Central North America (M_w ~ 7–8, New Madrid; Obermeier, 1996) triggered liquefaction. However, it should also be noted that there was no liquefaction reported during the Killari (Latur) earthquake (M 6.3) and 1997 Jabalpur earthquake (M 5.8) which show intensity XI and VIII on the MM scale, respectively. Thus, considering the extent of liquefaction and severity, the magnitude of the causative earthquake might have been > M_w 6.3.

5.6. Seismicity of the region

Historical and recent data suggest that a few earthquakes have occurred elsewhere in the vicinity of Palghat Gap since 1865, including a probable moderate event felt near Coimbatore in 1900 (e.g., Basu, 1964; Rajendran and Rajendran, 1996; Rajendran et al., 2009; Fig. 2). The epicentral intensity of this earthquake (M 6.0) has been calculated as VII on MM scale (Basu 1964) and the epicentre is located ~ 70 km from the present study area. Of late there is an increase in the number of minor earthquakes in this region during the last two decades, which has prompted evaluation of several local seismogenic faults. Several historical earthquakes (M ≤ 5.0) have been reported in the vicinity of the study region, which include the ones that occurred in the years 1833, 1856 (Oldham, 1883) and in 1953 (Gopal, 1953). The 1988 Idukki earthquake (Singh et al., 1989; Rastogi et al., 1995) and the twin events of 2000 and 2001in Erattupeta/Pala are the contemporary examples of earthquakes in this region (Rastogi, 2001; Bhattacharya and Dattatrayam, 2002; see Fig 2). The last mentioned is the largest size event that has occurred in recent history (Rajendran and Rajendran, 2009). The 12 December 2000 Erattupettah earthquake (ML 5.0) with recorded intensity VI on the MM scale, in the epicentral area did not show any evidence of liquefaction. Based on their studies Rajendran et al. (2009) suggest that the central midland region must be considered as seismically most potential region in Kerala.

The 2nd December 1994 Wadakkancheri earthquake (M_w 4.3) was the largest one that occurred in the study area in recent times (IMD, 1995; Rajendran and Rajendran, 1995). The epicentral intensity reported in this event is V on MM Scale. Subsequently, the seismic observatory established at Peechi (about 30 km from the epicentral area; Fig. 19) recorded several low-level seismicity in this area (Rajendran et al., 2009; Singh et al., 2016a; Singh et al., 2016b). This may suggest that the present study area is close to a potential seismic source zone for earthquakes and the ongoing low-level seismicity could be inter-seismic as most of them are falling in the hanging wall side of the Desamangalam fault (Fig. 19).

6. Conclusions

The peninsular India has a low rate of modern seismicity and historically very few records of damaging earthquakes. The 1993 Killari (Latur), the 1997 Jabalpur and the 2001 Bhuj earthquakes are the most significant events in the recent past (Rajendran and Rajendran, 2020). These events are said to be the associated with reactivation of preexisting structures with long return periods (Rajendran et al., 1996; Khan et al., 2013; Rajendran and Rajendran 2020). The current hazard map is based exclusively on historical and instrumentally recorded seismicity. However, the low rate and short historical records make it difficult to predict the earthquake hazard scenario for peninsular India, which exhibits long and aperiodic recurrence intervals. One approach to address this problem entails the use of paleoseismological tools to constrain the occurrence of prehistoric earthquakes. Such studies in the last 30 years have further improved our ability to interpret the pre-historic earthquake record, especially in the cratonic regions, characterized by infrequent earthquakes.

In the present study, we evaluated the Holocene stratigraphy from the shallow sedimentary sections along the valleys/paleochannels observed on the southern side of the main trunk of the Bharathapuzha River. These sections show preserved sedimentary clues for seismic as well as climatic events (Fig. 19). The silty sand units observed in the channels may indicate that they were active at least until ~ 2 ka years. The oldest unit exposed in the trench is dated at 10.7 ± 0.9 ka. The 5–6 ka BP peat bed, possibly a part of a regional climatic event, is also identified from this area. The liquefaction features are identified from an area of about 100 sq km with the source beds occurring below 2.5 m. We have tried to estimate causative earthquakes in terms of intensity and magnitude from the empirical relations available. The results suggest an VIII intensity on the ESI-2007 scale could have occurred in the epicentral area to produce the recorded liquefaction effects in an area of about 100 sq km. The earthquakes 1819 Allah Bund (M_w 7.6-8.0; Rajendran and Rajendran, 2001; Naik et al., 2020; Sunilkumat et al., 2024) and 2001 Bhuj earthquake (M_w 7.7; Bodin and Horton, 2004) were calculated to have an epicentral intensity of XI on the ESI-2007 scale. Our estimate suggests a maximum magnitude of M_w ≈6.3 for the earthquake that generated liquefaction in the present study area and this conjecture is further supported by the fault-based studies conducted earlier in the area (John and Rajendran 2009).

Here, we report, for the first time, the multiple episodes of liquefaction induced by pre-historic earthquakes from a site s in southern peninsular India - a region of low-level seismicity. The evidence of liquefaction, triggered by past earthquakes, is discovered within the topmost level of the sections and is mostly younger than 2 ka. The observations suggest both hydraulic fracturing and lateral spread for the formation of sand dikes. The liquefaction field spread over an area of about 100 sq. km could have been caused by a moderate event (M_w 5.5–6.5) from a nearby source. The chronological inputs suggest that the older event event occurred between 2 and 2.5 ka BP. f The younger event (780-year BP) warrants further studies for bracketing the event window. The studies elsewhere suggest the necessity of more regional studies to improve the constraints on the sizes and timings of liquefaction events (Tuttle 2001). We also recommend crustal deformation studies to understand the behaviour of the causative fault and its segmentation, if any. However, since this zone is close to a seismogenic structure, this area is eligible to be included as one of the potential source zones of moderate earthquakes.

Aside from constraining the earthquake recurrence, the identification and characterization of paleoliquefaction can provide valuable insights into the liquefaction processes in the impacted area. Such phenomena can cause severe damage to buildings, infrastructure, and loss of life. Therefore, conducting a thorough liquefaction potential analysis of the area is of utmost importance to zero in on high-risk zones and implement appropriate mitigation measures. The study presented here introduces a methodology applicable to the cratonic areas elsewhere in the world characterized by infrequent earthquakes and low levels of seismic preparedness.

CRediT authorship contribution statement

Biju John: Writing – review & editing, Writing – original draft, Visualization, Validation, Supervision, Resources, Project administration, Methodology, Investigation, Funding acquisition, Formal analysis, Data curation, Conceptualization. **Yogendra Singh:** Writing – review & editing, Software, Project administration, Investigation, Data curation. **C.P Rajendran:** Writing – review & editing, Visualization, Validation.

Declaration of competing interest

The authors declare that they have no known competing financial interests or personal relationships that could have appeared to influence the work reported in this paper.

Acknowledgments

This work is funded by the Department of Science and Technology, Government of India (SR/S4/ES-434/2009). We thank the Director of the National Institute of Rock Mechanics, Bangalore for providing the institutional facilities. We thank Ananya Divyadarshini, Associate Professor, Department of Geology, Utkal University, Odisha for her suggestions and corrections on the earlier drafts. We are thankful to the reviewers for the critical reviews of the manuscript and helpful suggestions to improve the paper.

Appendix A. Supplementary data

Supplementary data to this article can be found online at https://doi.org/10.1016/j.jseaes.2024.106373.

Data availability

Data will be made available on request.

References

Alappat, L., Frechen, M., Tsukamoto, S., Anupama, K., Prasad, S., Gopakumar, P.G., Sree Kumar, S., 2021. Evidences of early to mid-Holocene land–sea interactions and formation of Wetlands of Central Kerala in the southwest coast of India. Reg. Stud. Mar. Sci. 48. https://doi.org/10.1016/j.rsma.2021.102009.

Ambraseys, N.N., 1988. Engineering seismology: part I. Earthq. Eng. Struct. Dyn. 17 (1), 1–50.

Ambraseys, N.N., Jackson, J.A., 1998. Faulting associated with historical and recent earthquakes in the Eastern Mediterranean region. Geophys. J. Int. 133 (2), 390–406.

Arogyaswami, R.N.P., 1962. The origin of the Palghat Gap. Rec. Geol. Surv. India 93, 129–134.

Basu, K.L., 1964. A note on the Coimbatore earthquake of 8th February 1900. Indian J. Meteorol. Geophys. 15, 281–286.

Bhaskar Rao, Y.J., Kelley, S.P., Harris, N., Narayana, B.L., Srikatappa, C., 2006. An 40Ar–39Ar laser-probe study of pseudotachylites in charnockite gneisses from the Cauvery Shear Zone system, South India. Gondwana Res. 10 (3), 357–362. https://doi.org/10.1016/j.gr.2006.02.005.

Bhattacharya, S.N., Dattatrayam, R.S., 2002. Earthquake sequences in Kerala during December 2000 and January 2001. Curr. Sci. 82, 1275–1278.

Castilla, R.A., Audemard, F.A., 2007. Sand blows as a potential tool for magnitude estimation of pre-instrumental earthquakes. J. Seismol. 11, 473–487.

Collins, C., Cummins, P., Clark, D., Tuttle, M., Arsdale, R.V., 2004. Paleoliquefaction studies in Australia to constrain earthquake hazard estimates. NZSEE Conference Paper No. 50, 7p.

Copley, A., Mitra, S., Sloan, R.A., Gaonkar, S., Reynolds, K., 2014. Active faulting in apparently stable peninsular India: Rift inversion and a Holocene-age great earthquake on the Tapti Fault. J. Geophys. Res. 119. https://doi.org/10.1002/2014JB011294.

D'Cruz, E., Nair, P.K.R., Prasannakumar, V., 2000. Palghat gap— a dextral shear zone from the south Indian granulite terrain. Gondw. Res. 3, 21–31.

Drury, S.A., Harris, N.B.W., Holt, R.W., Reeves-Smith, G.J., Wightman, R.T., 1984. Precambrian tectonics and crustal evolution of south India. J. Geol. 92, 3–20.

Frakes, L.A., Kemp, E.M., 1972. Influence of continental positions on early tertiary climates. Nature 240, 97–100.

Galli, P., 2000. New empirical relationships between magnitude and distance for liquefaction. Tectonophysics 324 (3), 169–187.

Galli, P., Ferreli, L., 1995. A methodological approach for historical liquefaction research. In: Perspectives in Paleoseismology, vol. 6. Association of Engineering Geologists Special Publication, pp. 35–48.

Ghosh, J.P., de Wit, M.J.S., Zartman, R.E., 2004. Age and tectonic evolution of Neoproterozoic ductile shear zones in the Southern Granulite Terrain of India, with implications for Gondwana studies. Tectonics 23, TC3006. https://doi.org/10.1029/2002TC001444.

Gopal, V., 1953. A note on the investigations into the recent earthquake shocks in Kottayam District. Unpublished report, Geological Survey of India, Kolkata, Travancore-Cochin, p. 6p.

Green, R.A., Bommer, J.J., 2019. What is the smallest earthquake magnitude that needs to be considered in assessing liquefaction hazard? Earthq. Spectra 35 (3), 1441–1464.

GSI, 2000. Seismotectonic atlas of India and its Environs, GSI Special publication no. 59.

GSI, 2019. Geological map-1:2M Bhukosh-GSI. https://bhukosh.gsi.gov.in/Bhukosh/Public (accessed on February 5, 2024).

Gutenberg, B., Richter, C.F., 1956. Earthquake magnitude, intensity, energy, and acceleration: (second paper). Bull. Seismol. Soc. America 46 (2), 105–145.

Holzer, T., Clark, M.M., 1993. Sand boils without earthquakes. Geology 21, 873±876.

Holzer, T.L., Jayko, A.S., Hauksson, E., Fletcher, J.P.B., Noce, T.E., Bennett, M.J., Dietel, C.M., Hudnut, K.W., 2010. Liquefaction caused by the 2009 Olancha, California (USA), M5.2 earthquake. Eng. Geol. 116, 184–188.

IMD, 1995. Report on microearthquake survey in Trichur District. Kerala 18.

John, B., Divyalakshmi, K.S., Singh, Y., Srinivasan, C., 2013. Use of SRTM data for a quick recognition of the active tectonic signatures. Int. Semin. Geomorph. 2013, O91–O94.

John, B., Babu, A.R., Subrahmanyam, D.S., Singh, Y., Divyalakshmi, K.S., Praseeda, E., Samui, P., Ganapathy, G.P., 2016. Seismicity of Kerala: An update. RARE 2016 Published by Atlantis Press, 217-220.

John, B., Rajendran, C.P., 2008. Geomorphic indicators of Neotectonism from the Precambrian terrain of peninsular India- A study from the Bharathapuzha Basin, Kerala. J. Geol. Soc. India 71, 827–840.

John, B., Rajendran, C.P., 2009. Evidence of episodic brittle faulting in the cratonic part of the Peninsular India and its implications for seismic hazard in slow deforming regions. Tectonophysics 471, 240–252.

Johnston, A.C., Kanter, L.R., 1990. Earthquakes in stable continental crust. Sci. Am. 262, 68–75.

Johnston, A.C., 1989. Seismicity of stable continental interiors, In S. Gregersen and P.W. Basham (Eds.) Earthquakes at north Atlantic passive margins: Neotectonics and post glacial rebound Kluwer Academic publishers, 299-327.

Khan, P.K., Mohanty, S.P., Sinha, S., 2013. Recurrence of Moderate to large earthquakes in Peninsular India with special reference to 2001 M_w 7.3 Bhuj Event. In: In: Conference on Modern Geological and Geophysical Methods and Their Applications, p. 99.

Kumar, S., Wesnousky, S.G., Rockwell, T.K., Briggs, R.W., Thakur, V.C., Jayangondaperumal, R., 2006. Paleoseismic evidence of great surface rupture earthquakes along the Indian Himalaya. J. Geophys. Res. 111, B03304. https://doi.org/10.1029/2004JB003309.

Lowe, D.R., 1975. Water escape structures in coarse-grained sediments. Sedimentology 22, 157–204.

Lunina, O.V., Gladkov, A.S., 2015. Seismically induced clastic dikes as a potential approach for the estimation of the lower bound magnitude/intensity of paleoearthquakes. Eng. Geol. https://doi.org/10.1016/j.enggeo.2015.06.008.

Mallikarjuna, C., Vidyadharan, K.T., Pawar, S.D., Senthiappan, M., Francis, P.G., 1980. Geological, Geochemical and Geotechnical aspects of the laterites of Kerala, In: proceedings of the international seminar on laterization process, 425-435.

McCalpin, J.P., 2009. Paleoseismology. Int. Geophys. Ser. 95, 613P.

Michetti, A.M., Esposito, E., Guerrieri, L., et al., 2015. Environmental Seismic Intensity scale - ESI 2007. Mem Descr. Carta Geol. D'lt XCVII 11–19.

Naik, S.P., Mohanty, A., Porfido, S., Tuttle, M., Gwon, O., Kim, Y.-S., 2020. Intensity estimation for the 2001 Bhuj earthquake, India on ESI-07 scale and comparison with historical 16th June 1819 Allah Bund earthquake: A test of ESI-07 application for intraplate earthquakes. Quat. Int. 536, 127–143.

Newbold, C., 1846. Summary of geology of southern India. J. R. Asiat. Soc. G. B. Irel. 8, 251.

Obermeier, S.F., 1996. Use of liquefaction-induced features for Paleoseismic analysis: an overview of how seismic liquefaction features can be distinguished from other features and how their regional distribution and properties of source sediment can be used to infer the location and strength of Holocene Paleo-earthquakes. Eng. Geol. 44, 1–76.

Obermeier, S.F., Olson, S.M., and Green, R.A., 2005. Field occurrences of liquefaction-induced features: a primer for engineering geologic analysis of paleoseismic shaking. Eng. Geol. 76(3-4), 209–234. *https:*doi.org/10.1016/j.enggeo. 2004.07.009.

Oldham, R.D., 1883. A catalogue of Indian earthquakes from the earliest to end of AD 1869. Memoir Geol. Survey India 19 (3), 1–53.

Owen, G., 1987. Deformation processes in unconsolidated sands. In Deformation of Sediments and Sedimentary Rocks; Jones, M.E., Preston, R.M.F., Eds.; Geological Society of London Special Publication 29, 11–24.

Paul Bodin, Steve Horton; Source Parameters and Tectonic Implications of Aftershocks of the M_w 7.6 Bhuj Earthquake of 26 January 2001. Bulletin of the Seismological Society of America 2004;; 94 (3): 818–827. doi: https://doi.org/10.1785/0120030176.

Praseeda, E., John, B., Srinivasan, C., Singh, Y., Divyalakshmi, K.S., Samui, P., 2015. Thenmala fault system, southern India: Implication to Neotectonics. J. Geol. Soc. India 86, 391–398.

Rajendran, C.P., Singh, T., Mukul, M., Thakkar, M., Kothyari, G.C., John, B., Rajendran, K., 2020 Paleoseismological Studies in India (2016-2020): Status Prospects Proc. Ind. Nat. Sci. Acad. 86 (1), 585-607.

Rajendran, C.P., Rajagopalan, G., Narayanaswamy,, 1989. Quaternary geology of Kerala: evidence from radiocarbon dates. J. Geol. Soc. India 33 (3), 218–222.
Rajendran, K., Rajendran, C.P., 1995. A report on the December 2, 1994 Earthquake. Technical Report, Centre for Earth Science Studies, p. 34p.
Rajendran, C.P., Rajendran, K., 1996. Low moderate seismicity in the vicinity of Palghat gap, south India and its implication. Curr. Sci. 70, 304–307.
Rajendran, C.P., John, B., Sreekumari, K., Rajendran, K., 2009. Reassessing the earthquake hazard in Kerala based on historical and current seismicity. J. Geol. Soc. India 73, 785–802.
Rajendran, C.P., John, B., Rajendran, K., Sanwal, J., 2016. Liquefaction record of the great (1934) earthquake predecessors from the north Bihar alluvial plains of India. J. Seismol. 20, 733–745. https://doi.org/10.1007/s10950-016-9554-z.
Rajendran, C.P., Rajendran, K., 2001. Characteristics of deformation and past seismicity with the 1819 Kutch earthquake, northwestern India. Bull. Seismol. Soc. Am. 91, 407–426.
Rajendran, C.P., Rajendran, K., 2022. Earthquakes of the Indian subcontinent seismotectonic perspectives. Springer. 253P.
Rajendran, C.P., Rajendran, K., John, B., 1996. The 1993 Killari (Latur), Central India earthquake: an example of fault reactivation in the Precambrian crust. Geology 24, 651–654.
Ramakrishnan, M., 1993. Tectonic evolution of the granulite terrains of southern India. Memoir Geol. Soc. India 25, 35–44.
Rao, T.K.G., Rajendran, C.P., Mathew, G., John, B., 2002. Electron spin resonance dating of fault gouge from Desamangalam, Kerala: evidence for Quaternary movement in Palghat gap shear zone. Proc. Indian Acad. Sci. Earth Planetary Sci. 111, 103–113.
Rastogi, B.K., 2001. Erattupettah earthquake of 12 December 2000 and seismicity of Kerala. J. Geol. Soc. India 57, 273–274.
Rastogi, B.K., Chadha, R.K., Sarma, C.S.P., 1995. Investigations of June 7, 1988 earthquake of magnitude 4.5 near Idukki Dam in southern India. Pure Appl. Geophys. 145, 109–122.
Seed, H.B., Idriss, L.M., 1982. Ground Motions and Soil Liquefaction during Earthquakes, Earthquake Engineering Research Institute, University of California, Berkeley, 134 p.
Serva, L., Vittori, E., Comerci, V., et al., 2016. Earthquake Hazard and the Environmental Seismic Intensity (ESI) Scale. Pure Appl. Geophysics 173, 1479–1515.
Shajan, K.P., 1998. Studies on late Quaternary sediments and sea level changes of the central Kerala coast, India, CUSAT, Unpublished PhD thesis.
Sibson, R.H., 1989. Earthquake faulting as a structural process. J. Struct. Geol. 11, 1–14.
Singh, Y., John, B., Ganapathy, G.P., 2016a. Geomorphic studies for identification of active fault: observations from smaller river basins, South India, RARE 2016. Published by Atlantis Press 221–226.
Singh, Y., John, B., Ganapathy, G.P., George, A., Harisanth, S., Divyalakshmi, K.S., Kesavan, S., 2016b. Geomorphic observations from the southwestern terminus of Palghat Gap, south India and their tectonic implications. J. Earth Syst. Sci. 125, 821–839. https://doi.org/10.1007/s12040-016-0695-9.
Singh, H.N., Raghavan, V., Varma, A.K., 1989. Investigation of Idukki earthquake sequence of 7th–8th June 1988. J. Geol. Soc. India 34, 133–146.
Subramaniam, K.S., Muraleedharan, M.P., 1985. Origin of the Palghat Gap in South India—a synthesis. J. Geol. Soc. India 26, 28–37.
Świątek, S., Belzyt, S., Pisarska-Jamroży, M., & Woronko, B. (2023). Sedimentary records of liquefaction: Implications from field studies. J. Geophys. Res.: Earth Surf., 128, e2023JF007152. https://doi. org/10.1029/2023JF007152.
Sunilkumar, T.C., Zhang, Z., Wang, Z., Wang, W., He, Z., 2024. ***Unveiling the mechanisms of the 1819 M 7.7 Kachchh Earthquake, India: Integrating physicsbased simulation and strong ground motion estimates***. Earth and Space Science 11, e2023EA003308. https://doi.org/10.1029/2023EA003308.
Sykes, L.R., 1978. Intraplate seismicity, reactivation of preexisting zones of weakness, alkaline magmatism, and other tectonism postdating continental fragmentation. Rev. Geophys. 16 (4), 621–688.
Tuttle, M.P., 2001. The use of liquefaction features in paleoseismology: Lessons learned in the New Madrid seismic zone, central United States. J. Seismol. 5, 361–380.
Wells, D.L., Coppersmith, K.J., 1994. New empirical relationships magnitude, rupture length, rupture width rupture area and surface displacement. Bull. Seismol. Soc. Am. 84, 974–1002.